Paleoclimate in continental northwestern Europe during the Eemian and eEarly -Weichselian (125-97 ka): insights from a Belgian speleothem.

Stef Vansteenberge[1], Sophie Verheyden[1,2], Hai Cheng[3,4], R. Lawrence Edwards[4], Eddy Keppens[1] and Philippe Claeys[1]

Correspondence to: S. Vansteenberge (svsteenb@vub.ac.be)

[1]Earth System Science Group, Analytical-, Environmental- & Geo-Chemistry, Vrije Universiteit Brussel, Brussels, Belgium
[2]Royal Belgian Institute for Natural Sciences, Brussels, Belgium
[3]Institute of Global Environmental Change, Xi'an Jiaotong University, Xi'an, China
[4]Department of Earth Sciences, University of Minnesota, Minneapolis, USA

Abstract. The Llast interglacial serves as an excellent time interval for studying climate dynamics during past warm periods. Speleothems have been successfully used for reconstructing the paleoclimate of lLast interglacial continental Europe. However, all previously investigated speleothems are restricted to southern Europe or the Alpsine region, leaving large parts of northwestern Europe undocumented. To better understand regional climate changes over the past, a larger spatial coverage of European Last Interglaciallast interglacial continental records is essential and speleothems, because of their ability to obtain excellent chronologies, can provide a major contribution.speleothems is essential. Here, we present new, high-resolution data from a stalagmite (Han-9) obtained from the Han-sur-Lesse Ceave in Belgium. The Han-9 formed between 125.3 and ~97 –ka, with interruptions of growth occurring at 117.3 – 112.9 -ka and 106.6-103.6 -ka. The speleothem was investigated for its growth, morphology and stable isotope ($\delta^{13}C$ and $\delta^{18}O$) compositioncontent. Speleothem formation within the Last Interglacial started relatively late in Belgium, as this is the oldest sample of that time period found so far, dated at The speleothem started growing relatively late within the last interglacial, at 125.3 –ka,. as Oother European continental archives suggest that Eemian optimum conditions were already present during that time.. therefore Iit appears that the initiation of the Han-9 growth is caused by an increase in moisture availability, linked to wetter conditions around 125.3 –ka. The $\delta^{13}C$ and $\delta^{18}O$ proxies indicate a period of relatively stable conditions after 125.3 –ka, however, at 120 ka the speleothem $\delta^{18}O$ registered the first signs of regionally changing climate conditions, being a modification of ocean source $\delta^{18}O$ linked to an increase in ice volume towards the Marine Isotope Stage (MIS) 5e-5d transition. At 117.5 ka, The end of the Eemian is marked by drastic vegetation changes are recorded byin the speleothemHan-9 $\delta^{13}C$ at 117.5 ka, immediately followed by a cessation ofstop in speleothem growth at 117.3 -ka, suggesting that climate became significantly dryera transition to significantly dryer conditions. The Han-9 record covering the eEarly -Weichselian displays larger amplitudes in both the isotope proxies and the changes in stalagmite morphology, evidencing increased variability compared to the Eemian. Greenland Stadials that appear to be analogous to those in Greenland are recognized in the Han-9 and the chronology is consistent with other European (speleothem) records. Greenland Stadial 25 is reflected as a cold/dry period within Han-9the stable isotope proxies and the second interruption in speleothem growth occurs simultaneously with Greenland Stadial 24.

Keywords.: paleoclimate, Last Interglaciallast interglacial, Eemian, northwestern Europe, speleothem, stable isotopes, millennial-scale variability, Greenland sStadials

1 Introduction

The ~~Last Interglacial~~last interglacial (LIG) period is known as the time interval before the l~~L~~ast g~~G~~lacial period during which temperatures were similar to or higher than those ~~present and the past~~ of the Holocene period and Present Day (Otto-Bliesner et al., 2013). In marine sediment cores, the LIG is defined as Marine Isotope Stage (MIS) 5e (Shackleton, 1969). The start and end of the MIS 5e period are conventionally set at 130 and 116 ka, respectively, based on marine records (e.g. Martinson et al., 1987). The expression of the LIG in continental western Europe is defined as the Eemian, although it does not coincide precisely with the isotopically constrained MIS 5e (Otvos, 2015). Given the ongoing debate about the ~~Last Interglacial~~ LIG nomenclature, clarification about the terms used in this manuscript is~~are~~ required. This study focusses on speleothem archives, thus the terms "Eemian" and "Weichselian" are preferred in the context of European continental paleoclimate. The Eemian is defined as the optimum or acme LIG climate conditions (the "sensu stricto" definition). Subsequent to the Eemian, the Weichselian starts, with the e~~E~~arly -Weichselian in continental records corresponding to the time-equivalent of MIS 5d – 5a. "Glacial inception" is considered to be informal and only marks the Eemian to e~~E~~arly -Weichselian transition.

The term "Eemian" was originally ~~defined~~ introduced by P. Harting ~~(~~in1875~~)~~ and was characterized by the occurrence of warm water mollusks in marine sediments of the Eem R~~r~~iver valley, near Amsterdam, the Netherlands ~~(Bosch et al., 2000)~~. Nowadays, the Eemian is mostly interpreted as an interval of warmer climate ~~amelioration~~ associated with the spread of temperate mixed forests in areas with similar vegetation to today (Kukla et al., 2002). However, the Eemian is also known to be a diachronous unit (Kukla et al., 2002; Wohlfarth et al. 2013), with a longer duration of up to 20 ka, from 130 to 110 ka, in southern Europe as evidenced by pollen records (Sanchez Goñi et al., 1999; Tzedakis et al., 2003). The LIG period exhibited global mean temperatures (GMT) 1.5° to 2° ~~–~~C higher than the pre-anthropogenic average together with peak eustatic sea levels that were between 5.5 and 9 ~~–~~m higher than present (Dutton and Lambeck, 2012). Therefore, the LIG gained a lot of attention from both paleoclimate and climate modelling communities for studying a warmer climate state and potential future sea-level rise (Loutre et al., 2014; Goelzer et al., 2015), even though the present-day configuration of Earth's orbital forcing parameters is~~was~~ different (Berger and Loutre, 2002). ~~Subsequent to~~Following the Eemian, climate went into a glacial mode known as the l~~L~~ast g~~G~~lacial cycle, or the Weichselian in the western European continental terminology, which lasted until the Holocene. A major ~~control~~feature of~~n~~ climate variability during the l~~L~~ast g~~G~~lacial is the occurrence of millennial ~~–~~scale~~d~~, rapid cold-warm-cold cycles, known as Dansgaard-Oeschger (D/O) events (Bond et al., 1993). These D/O cycles are expressed as alternating ~~succession~~ Greenland s~~S~~tadial (GS) and i~~I~~nterstadial (GIS) phases in Greenland ice cores (Dansgaard et al., 1993; NGRIP members, 2004)~~, as Atlantic Cold Events registered in sea surface temperature proxies.~~ Some of the s~~S~~tadials are also associated with an increased~~s~~ ~~in the~~ flux of i~~I~~ce r~~R~~afted d~~D~~ebris (IRD) in the North ~~-~~Atlantic O~~o~~cean (McManus et al., 1994). These events have been linked to changes in the strength and shifts in the northwards extent of ~~the~~ Atlantic Meridional Overturning Circulation (AMOC) (Broecker et al., 1985). The exact cause of such changes in the AMOC mode is~~are~~ still debated. Nevertheless, according to Barker et al. (2015), it is more likely a non-linear response of a gradual cooling of the climate than a result of enhanced fresh-water input by iceberg calving, as previously proposed by Bond et al. (1995) and van Kreveld et al. (2000). Likewise, continental pollen records extracted from cores of Eifel Maar lakes (Sirocko et al., 2005) or peat bogs in the Vosges, France (Woillard, 1978; de Beaulieu and Reille, 1992; de Beaulieu, 2010), have recorded changes in pollen assembly, attributed to D/O variability. So far, up to 26 GS's have been

identified in ice-cores, with GS 26 recognized as corresponding to the end of the Eemian i~~I~~nterglacial period (NGRIP members, 2004).

Speleothems ~~have often been used~~are ideal for ~~l~~Late -Quaternary paleoclimate studies because of their ability to~~of constructing~~obtain accurate chronologies with U/Th dating of up to 600 ka and their potential ~~of holding~~to yield high resolution~~,~~ (up to seasonal scale)~~,~~ paleoclimate records~~signals~~ (Fairchild and Baker, 2012). The speleothem records covering the Eemian and ~~E~~early -Weichselian in Europe have provided detailed paleoclimate reconstructions (Genty et al., 2013). Several speleothem stable isotope proxies from Europe record optimum climatic conditions during the Eemian (Meyer et al., 2008; Couchoud et al., 2009) and D/O climate events during the early Weichselian (Bar-Matthews et al., 1999; Drysdale et al., 2007; Boch et al. 2011)~~These have shown that Eemian optimum conditions are indeed registered in European speleothem stable isotope proxies (Meyer et al., 2008; Couchoud et al., 2009) and that D/O climate events are also recorded during the Early Weichselian (Bar-Matthews et al., 1999; Drysdale et al., 2007; Boch et al. 2011)~~. Yet so far, all records covering that time period are located in southern Europe (Italy, s~~S~~outhern France, Levant) or the Alps~~ine region~~. This study presents a new high-resolution speleothem dataset from Belgium ~~in order to~~that expands the European coverage of ~~Last Interglacial~~last interglacial speleothem archives northwards.

Earlier chronostratigraphic work on speleothem deposits and detrital sediments within Belgian caves marked the presence of glacial/interglacial cycles, with speleothem formation restricted to interglacial periods, when warm and wet climates favored growth. Detrital sediments settle in colder periods, with river deposits in cold wet periods and reworked loams during cold dry periods (Quinif, 2006). From the 1980's onwards, speleothems covering MIS 9 to 1 have been found in various Belgian caves (Bastin and Gewelt, 1986; Gewelt and Ek, 1988). Quinif and Bastin (1994) analyzed an Eemian flowstone from the Han-sur-Lesse C~~c~~ave for its pollen composition~~content~~, and ~~have shown~~demonstrated that vegetation above the cave area reflects interglacial climate optimum conditions around 130 +/- 10 ka. However, the dating of this material contains large uncertainties related to the alphaspectrometric methodology used. This study focusses on a recently obtained speleothem, ~~the~~ Han-9 from the Han-sur-Lesse C~~c~~ave in s~~S~~outhern Belgium. This ~~70 cm long~~ stalagmite was analyzed to better constrain 1) the chronology of Eemian optimum conditions in Belgium and 2) the occurrence and signature of millennial~~l (D/O)~~ scale~~d~~ climate variability (D/O) over northwestern Europe during the c~~E~~arly -Weichselian.

2 Han-sur-Lesse C~~c~~ave: geology and cave parameters

The Han-sur-Lesse C~~c~~ave system is the largest known subterranean karst network in Belgium, with a total length of ~10~~–~~km. It is located within the *Calestienne*, a SW-NE trending superficial limestone belt of Middle Devonian age. After deposition, these Paleozoic sediments underwent Hercynian folding followed by Mesozoic erosion. The current hydrographic network was established during the Neogene and Pleistocene, by erosion into these folded belts (Quinif, 2006). The cave system was formed within the *Massif du Boine*, part of an anticline structure consisting out of Middle to Late Givetian reefal limestones, by a meander shortcut of the Lesse R~~r~~iver (Fig. 1B). The thickness of the epikarst zone above the cave is estimated to be around 40 m.

The area of the Han-sur-Lesse C~~c~~ave is located ~~ca.~~ ~200 km inland at an elevation of 200 m above sea level~~.s.l.~~ (Fig. 1) and is marked by a maritime climate with cool summers and mild winters. For the period 1999-2013, average year-temperature above the cave was 10.2~~–~~°C and average yearly rainfall amount 820~~–~~mm ~~/year~~ $year^{-1}$~~,~~ ~~which~~The amount of precipitation does not follow a seasonal distribution ~~is spread over the entire year~~ (Royal

Meteorological Institute, RMI). The dominant moisture source in northwestern Europe is the North Atlantic Ocean, and this remains constant throughout the year (Gimeno, 2010). Modern $\delta^{18}O$ of rainfall seasonally varies between -17‰ in winter and -4‰ in summer (Van Rampelbergh et al., 2014). The area above the cave mainly consists ~~out~~ of C3 type vegetation with *Corylus*, *Fagus* and *Quercus* trees, and as a natural reserve it has been protected from direct human influence for over 50 years (Timperman, 1989). The Lesse River enters the cave system at the *Gouffre de Belveaux* and exits at the *Trou de Han* approximately 24 hours later. The Han-~~Stm~~-9 stalagmite was collected within the *Réseau Reénversé*, which is the most distal part of the *Réseau Sud* ~~or the southern network of the Han Sur Lesse cave system~~ (Fig. 1B). The natural connection between the *Réseau Sud* and~~with~~ other parts of the Han-sur-Lesse Ceave is fully submerged, but in 1960 an artificial tunnel was established facilitating ~~the~~ access~~ibility~~ (Timperman, 1989). When water of the Lesse River ~~water~~ is high, part of the stream is redirected through the *Réseau Sud*~~southern network~~ but it does not reach the *Réseau Renversé* (Bonniver, 2010). ~~The *Réseau Renversé* does not contain a stream.~~ Earlier studies have shown that cave drip waters are mostly supplied by diffuse flow through the host rock (Bonniver et al., 2011; Van Rampelbergh et al., 2014). The Han-sur-Lesse Ceave is partly accessible for tourists, but because of the difficult access, the~~the~~ *Réseau Sud*~~southern network~~ is protected from any anthropogenic influence. ~~Short term~~ Tt~~t~~emperature logging for six months with an interval of two hours ~~in the southern network~~*Réseau Renversé* shows an average cave temperature of 9.45°C with a standard deviation < 0.02 °C, which reflect~~sing~~ the average temperature of 9.2 °C above the cave for 2013. Minimum and maximum temperatures were 9.39 °C and 9.51 °C, respectively (C. Burlet, pers. comm.). This shows that the temperature in the *Réseau Renversé* is constant through the year and that it reflects the average temperature above the cave. In contrast, recent cave monitoring in more ventilated parts of the cave indicated a temperature seasonality of 3 °C (Van Rampelbergh et al., 2014). For the *Réseau Renverse*, there are no indications that cave morphology changed significantly since the last interglacial. Han-9, the stalagmite presented in this study, was deliberately sampled because it was already broken into three parts, so no other speleothems had to be destroyed. Although the sample was broken, it was still in situ. The candle-shaped stalagmite has a length of 70cm (Fig. 2C-E).

The Han-sur-Lesse Ceave received scientific attention in the last decades, making it the best understood cave system in Belgium. This includes detailed hydrographic studies (Bonniver et al., 2010) and extended cave monitoring surveys (Verheyden et al., 2008; Van Rampelbergh et al., 2014), leading to successful paleoclimate reconstructions on Holocene speleothems down to seasonal scale (Verheyden et al., 2006; 2012; 2014; Van Rampelbergh et al., 2015). The elaborate cave monitoring (Fig. 1B) has provided a solid foundation ~~steady base~~ for understanding the cave system and to interpret its paleoclimate records, even back to ~120 ka.

3 Methods and analytical procedures

All ages were acquired by using U/Th dating at the University of Minnesota Earth Sciences Department, Minneapolis. Nine samples were analyzed in 2013 and an additional batch of 14 samples was dated in 2015 to further improve the age-depth model ~~and the time series,~~ with additional sampling locations selected ~~chosen in function of~~based on the preliminary age model and the stable isotope ($\delta^{13}C$ and $\delta^{18}O$) data (Fig. 2D). For all U/Th analyses, 150-200 mg of speleothem calcite was milled and analyzed with a Neptune multiple-collector plasma source mass spectrometer (MC-ICP-MS) from Thermo-Scientific ~~at the University of Minnesota. The used half-lives for ^{230}Th and ^{234}U are reported in Cheng et al. (2013). Ages were corrected assuming an initial $^{230}Th/^{232}Th$ ratio of 4.4 ±2.2 x 10^{-6}.~~The age datum is 1950 CE. ~~For additional information about the applied method, see Edwards et al. (1987) and Cheng et al. (2013) and references therein.~~ The applied method is based

Formatted: Font: Italic
Formatted: Font: Italic
Formatted: Font: Italic
Formatted: Font: Not Italic
Formatted: Font: Not Italic
Formatted: English (U.S.)

on the fundamental principles of U-Th dating and mass spectrometry on carbonates provided by Edwards et al. (1987). For state of the art improvements on sample preparation, MC-ICP-MS protocols and ^{230}Th and ^{234}U half-live values, see Shen et al. (2012) and Chen et al. (2013) and references therein. Age-depth modeling was carried out using the StalAge algorithm of Scholz and Hoffmann (2011). All depths are expressed in 'mm dft' with dft being 'distance from top'.

All ~~For~~ stable isotope analysis were carried out at the Stable Isotope Laboratory, Vrije Universiteit Brussel.~~,~~ ~~a~~A total of 1118 samples were drilled with a Merchantek MicroMill, a computer steered drill mounted on a microscope. Samples were taken along the central growth axis~~,~~ to avoid possible effects of evaporation during calcite deposition (Fairchild et al., 2006). For all samples,~~ 300 µm~~ tungsten carbide dental drill bits with a diameter of 300µm from Komet were used. As a~~In~~ function of the growth rate, 1000, 500 and 250-µm sampling resolutions were applied in order to maintain a more or less equal resolution in the time domain. For sample locations, see ~~Fig.~~Fig. 2D. Samples were kept at 50°C prior to analysis to avoid contamination. $\delta^{13}C$ and $\delta^{18}O$ isotope measurements were performed on a Perspective IRMS from Nu Instruments, coupled to a Nucarb automated carbonate preparation system and a minor amount (<100) on a Kiel III device coupled to a Delta plus XL from Thermo-Scientific. Two samples of the in-house standard MAR-2(2), made from Marbella limestone and which has been calibrated against the international standard NBS-19 (Friedman et al., 1982), were measured every 10 samples to correct for instrumental drift. Reported values for the MAR-2(2) are 0.13 ‰ Vienna Pee Dee Belemnite (VPDB) for $\delta^{18}O$ and 3.41 ‰ VPDB for $\delta^{13}C$. Analytical uncertainties on standards from individual batches were ≤ 0.05 ‰ for $\delta^{13}C$ and ≤ 0.08 ‰ for $\delta^{18}O$ on the Nu Instruments setup. At regular intervals,~~Every eight samples~~ a replicate sample~~double~~ was measured in a different batch to check for the reproducibility of the analytical method. Outliers were manually detected, removed and re-measured if sufficient material was present. ~~To check for isotopic equilibrium conditions during speleothem formation, nine Hendy tests (Hendy, 1971) consisting of 10 measurements, five at each lateral side, were carried out.~~ In addition, six 30 µm thin-sections were taken along the growth transect (Fig. 2D).

4 Results

4.1 Speleothem morphology

Figures 2C–2E show the interpretation of the internal morphology of ~~the~~ Han-9. In the lower part of the speleothem, below~~up to~~ 365 mm dft, ~~layering is extremely good~~the calcite was well-laminated alternating ~~expressed and consists of sub millimeter sized alternations of~~between thick white~~r~~ and slightly darker layers~~calcite~~. In the lower 15mm~~At the very base~~, some fine, brown detrital laminae can be seen, although they are confined to the very base and the lateral sides of the stalagmite. From ~~Layering is visible up to~~ 430~~365~~ mm dft,~~.~~ ~~T~~the calcite becomes progressively coarser and layering less expressed ~~from around 430 mm dft onwards, where~~ with alternations between~~of~~ thicker parts of denser and coarser calcite ~~are present~~. Starting from 365 mm dft, the speleothem calcite has a very coarse appearance and layering is almost indistinguishable. This goes on until 304 mm dft, where a first discontinuity in growth, D1, appears. This discontinuity was identified macroscopically. After D1, 100 mm of speleothem is characterized by alternating bands of dense and dark brown calcite with coarser, white calcite. ~~Sometimes, subtle fine layering can be observed, mainly in the coarser parts or on the lateral sides.~~ Between 200 and 176 mm dft, a band of dense, brown calcite is present. Within this band, very fine laminae of red-brown material can be observed. This band ends with a second discontinuity, D2. ~~Stalagmite growth of the upper part starts with a growth axis tilted towards the right, however after 20 mm the axis recovers to its original upright position.~~Following D2, the axis of growth for the next 20mm is tilted to the

Formatted: Superscript
Formatted: Superscript
Formatted: Font: Not Italic
Formatted: Font: Not Italic
Formatted: Font: Not Italic
Formatted: Font: Not Italic
Formatted: Font: Not Italic
Formatted: Font: Not Italic
Formatted: Font: Not Italic
Formatted: Font: Not Italic
Formatted: Font: Not Italic
Formatted: Font: Not Italic

right. The entire upper section consists of dense and dark brown calcite, with little variation except for a coarser interval between 58 and 40 mm dft. Besides some subtle unconformities marked by the dashed lines in Fig. 2D, no internal layering is visible macroscopically present. The location of the Thin-sections locations were chosen as representative of the typical morphologies displayed in the stratigraphic log in Fig. 2E. Fabrics are described according to Frisia (2015). In all thin sections, the dominant fabric of the calcite crystals was columnar (Fig. 3A). The layering, although often very well displayed macroscopically, was not distinguishable within the thin sections. Variations in fabric occur between macroscopically defined 'denser' and 'coarser' calcite (Fig. 2E), where the latter has smaller columnar calcite crystals with significantly more inter-crystalline porosity often filled with fluid inclusions (Fig. 3B), and thereby described as columnar open. The denser morphology has substantially larger crystals with almost no pore space and can be defined as columnar elongated. Another type of fabric occurs within the dark brown band of dense calcite between 200 and 176 mm dft. There, the columnar fabric is replaced with smaller more equant calcite crystals (Fig. 3C). which are then followed by a fine layer of brown detrital material representing D2.

4.2 U/Th dating

The results of U/Th datings are shown in Table 1. Dating samples are labeled by "DAT-X", with X representing the sample number in Fig. 2D. All ages are displayed as "ka". Atomic $^{230}Th/^{232}Th$ ranges between 1064 and 33652 × 10^{-6}. Because detrital Th is relatively low in all samples, ages were corrected assuming an initial bulk earth $^{230}Th/^{232}Th$ atomic ratio of 4.4 ±2.2 × 10^{-6}. Errors are given as 2σ and range between ±212 years and ±666 years. The U and Th concentrations determined in the 2013 samples allowed reduction of the sample size, resulting in smaller errors for the 2015 samples. From 672 to 176 mm dft, all ages are stratigraphically consistent; no age inversions occur when taking into account the 2σ error of the U/Th ages. Between 176 and 0 mm dft, the distribution of the ages is more chaotic, with the occurrence of several age inversions and outliers.

4.3 Stable isotopes: $\delta^{13}C$ and $\delta^{18}O$

Figures 2A and B show the results of the $\delta^{13}C$ and $\delta^{18}O$ analyses, plotted against sample depth in mm dft. All values are expressed in ‰ VPDB. The $\delta^{13}C$ varies between -3.58 and -10.30 ‰, with an average of -7.53 ‰. The $\delta^{18}O$ values show smaller variations, between -5.04 and -7.02 ‰, and with an average of -5.91 ‰. Lower amplitude variability in both $\delta^{13}C$ and $\delta^{18}O$ occur in the lower part of the stalagmite, and larger amplitude variations are present from ~400 mm dft upwards, corresponding to distinct transitions in morphology (alternating zones of dense, more brown and coarser, more white calcite, Fig. 2E).

To check whether the speleothem calcite was formed in isotopic equilibrium with the drip water, nine Hendy tests were carried out over the entire stalagmite (Fig. 2D). The results are shown in Fig. 4. First of all, $\delta^{18}O$ tends to be rather variable along a single growth layer, with variations up to 0.3 ‰. Nevertheless, this is still well below a threshold value of 0.8 ‰ (Couchoud et al., 2009; Gascoyne, 1992). Further, no significant covariation between the $\delta^{13}C$ and $\delta^{18}O$ records along the layers can be observed, except maybe slightly for Hendy test 8 and 2. However, the most valuable indication that the speleothem calcite was formed under (at least) near-

~~equilibrium conditions is given by a very low R^2 of 0.0387 between the $\delta^{13}C$ and $\delta^{18}O$ variations along the central growth axis of the speleothem, pointing towards no significant covariance between the two stable isotope proxies (Fig. 2A and 2B).~~

5~~.~~ Discussion

5.1 Age model

The StalAge algorithm (Scholz and Hoffmann, 2011) was applied to the individual ages in order to construct an age-depth model, displayed in Fig. 4~~5~~. It is clear that the stalagmite endured three separate growth phases, and that the discontinuities, expressed in the stalagmite morphology at 302 and 176mm dft (Fig. 2D), correspond to two hiatuses separating these three growth phases. In the first growth phase, all ages are in stratigraphic order and are included within the model and the 2σ error. DAT-1 has only limited weight in the final model and an explanation for this is given in the algorithm specifications (Scholz and Hoffmann, 2011). During the modeling process, the StalAge algorithm has a step where the data is screened for the occurrence of minor outliers and age inversions. This is done by fitting error weighted straight lines through subsets of three adjacent data points. However, DAT-1 is located in the basal part of the stalagmite, so less subsets of three data points can be used including DAT-1. If DAT-1 does not fit on the error weighted straight line created with the adjacent data points DAT-10 and DAT-11, which is the case here, the error of DAT-1 will be increased and the weight of DAT-1 in the Monte Carlo simulation for the age fitting will decrease. This results in less solutions where DAT-1 is included in the Monte Carlo simulated age models. The occurrence of substantial changes in growth rate in the boundary areas of a speleothem sample is recognized as a limitation of the StalAge algorithm (Scholz and Hoffmann, 2011). ~~For the U/Th dates obtained between 0 and 176 mm dft, errors had to be enlarged to 2000 years, to account for the occurrence of age inversions, resulting in increased errors calculated in the final age-depth model. This makes the model unreliable for this part, however, it is correct the assume a general time window for the growth of this upper part between ~104 and ~97 ka. Despite the problems with the upper 176 mm of the stalagmite, valuable information could be retrieved from the age-depth model. It is clear that the stalagmite endured 3 separate growth phases, and that the discontinuities, expressed in the stalagmite morphology at 302 and 176 mm dft (Fig. 2D), correspond to two hiatuses separating these 3 growth phases.~~ Even though the three growth phases were modeled separately with StalAge, the model does not perform well with the start of the Hiatus 2, as DAT-19 is completely excluded. Likely, this is again caused by the fact that DAT-19 is located in a boundary area. Here, the stalagmite petrography shows clear evidence of a significantly decreased growth rate after DAT-16 (110.6 ka), i.e. very dense, brownish calcite with fine laminae (Fig. 2C and E). In complex cases, such as in this study where multiple hiatuses occur, the simplest model is still the best. Therefore, linear interpolation combined with good observations of changes in petrography, was applied to include DAT-19 within the age model (Fig. 4, red line). For the third growth phase, because of the occurrence of several age inversions, the resulting age model is unreliable. Despite the fact that ages clearly cluster between ~103 and ~97 ka, the chronology of the third growth phase is only poorly constrained and therefore a detailed interpretation of Han-9 in terms of paleoclimate is limited to the first two growth phases.~~A second adjustment of the age-depth model had to be made at the end of growth phase 2. Morphologic evidence, being the dense, brown calcite with very fine laminae, points towards a decreased growth rate between 200 mm and 176 mm dft, and thus there is no evidence that the age of DAT-19, taken at 179 mm dft, should be considered as an outlier. Even if a higher detrital Th content would disturb the outcome of DAT-19, this would result in an older age.~~

~~Therefore, the result of the StalAge model was replaced with a linear interpolation between DAT-19 and DAT-16, taken at 201 mm dft (red line in Fig. 5).~~

The first ~~and oldest~~ growth phase starts at 125.34 +0.78/-0.66 ka with stable growth-rate of 0.02 mm yr^{-1} up to around 120.5 ka. After that, the growth rate significantly increases, with values up to 0.15 mm yr^{-1}. At 117.27 +0.69/-1.02 ka, growth ceases and the first hiatus, H1, starts. The hiatus lasts 4.41 +1.10/-1.49 ka and at 112.86 +0.47/-0.41 ka growth phase 2 starts. DAT-4 and DAT-5 were taken 6 mm below and above the discontinuity and the age-depth model does not show any reason to question the timing of H1. As for the second growth phase~~growth phase 2~~, growth-rate remains at a constant pace of 0.04 mm yr^{-1} until approximately 110.5 ka, where it decreases to 0.006 mm yr^{-1}. At 106.59 +0.21/-0.22 ka, the second growth phase ends~~. This hiatus (H2) lasts 3.0 +1.58/-1.28 ka, until 103.59 ka. Speleothem formation then completely comes to a hold at 97,22 +1.02/-2.61 ka~~. Given this age-depth model, stable isotopes were analyzed with a~~n average~~ temporal resolution between 100 and 0.3 years, and an average of 16 years.

5.2 Interpretation of stable isotope proxies

Comment [S1]: Structure of the stable isotope interpretation changed: subdivision between isotopic equilibrium, d13C and d18O. Isotopic equilibrium discussion was added since the Hendy tests are left out in the revised version. Here, the Pearson's correlation tests are discussed.

Formatted: Font: Bold

5.2.1 Isotopes deposited in isotopic equilibrium?

The best test for the presence of kinetic fractionation is to have a reproducible record (Dorale and Liu, 2009). However, in the absence of a second stalagmite record, Hendy tests could be performed (Hendy, 1971). The problem here is that growth rates are rather low and the layering very fine, so it would be hard to sample precisely in one layer. Therefore, an additional test for correlation of $\delta^{13}C$ and $\delta^{18}O$ was done by calculating the Pearson's correlation coefficient on the entire record and on the three growth phases separately (Table 2). Yet, a correlation between $\delta^{13}C$ and $\delta^{18}O$ does not give conclusive evidence for the presence of kinetic fractionation, as both $\delta^{13}C$ and $\delta^{18}O$ are expected to be controlled by climate and could therefore show positive or negative covariation (Dorale and Liu, 2009). The Pearson's coefficients reveal that there is a clear difference between the separate growth phases. The first growth phase, with $\rho = 0.024$, marks no covariation. The second growth phase, with $\rho = -0.467$, has a substantial degree of negative covariation, whereas the third growth phase ($\rho = 0.461$) has a positive covariation. The differences between the coefficients of the separate growth phases indicate that several processes are controlling the stable isotope variability and that the presence or absence of covariation reflects changes in climate conditions between the growth phases rather than the presence or absence of equilibrium. Nevertheless, equilibrium deposition between the drip water and recent calcite in Han-sur-Lesse Cave has been observed by Van Rampelbergh et al. (2014). ~~Stable isotope time series are displayed in Fig. 6.~~

Formatted: Superscript

Formatted: Superscript

Formatted: Superscript

Formatted: Superscript

Formatted: Superscript

Formatted: Superscript

5.2.2 Variations in speleothem $\delta^{13}C$

Comment [S2]: The entire section of δ13C has been modified according to the reviewers comments and the authors response.

Formatted: Font: Bold

Formatted: Font: Bold, Superscript

Formatted: Font: Bold

Formatted: Superscript

Formatted: Superscript

Formatted: Superscript

Formatted: Superscript

The $\delta^{13}C$ in Han-9 is controlled by changes in vegetation assembly above the cave. This is deduced from the match between Han-9 $\delta^{13}C$ and the abundance of grass pollen in the assembly of Sirocko et al. (2005) recovered from the Eifel maar (Fig. 1A and Fig. 5). The agreement between Han-9 $\delta^{13}C$ and the Eifel pollen assembly is remarkable; increases in $\delta^{13}C$ occur when the percentage of grass pollen increases in the Eifel record. Similar shifts in grass/forest vegetation have even been observed the Vosges region, France, 300km further south (Woillard, 1978; de Beaulieu and Reille, 1992; de Beaulieu, 2010) and in other records from northern and central

Europe (Helmens, 2014 and references therein). Also, the $\delta^{13}C$ of recent calcite formed with a current forest-type vegetation above the cave is ~-8‰ (Table 3). These values are similar to those observed during the last interglacial in Han-9 (125.3-117.3 ka, Fig. 5). Changes in $\delta^{13}C$ of several per mil are often attributed to changes in C3 versus C4 plants (McDermott, 2004). However, a higher abundance of grasses does not necessarily result in an increased amount of C4 vegetation. First of all, C4 species only make up ~1% of the total amount of vascular plant species in northwestern Europe today (Pyankov et al., 2010). Secondly, C4 species dominantly occur in a warmer, tropical climate (Ehleringer et al., 1997). Finally, within the subfamily of the Poideae, commonly referred to as the cool-season grasses and thriving in temperate European climate, all species use the C3 pathway (Soreng et al., 2015). The reason why speleothem calcite tends to be enriched in ^{13}C when vegetation is dominated by grasses is because grasses have a smaller biomass than trees and also the amount of soil respiration is lower, both leading to a smaller fraction of biogenic CO_2 compared to (heavier) atmospheric CO_2 within the soil (Genty et al., 2003). The similarity between the two records does not seem to hold up after 109 ka. From here on, $\delta^{13}C$ becomes more depleted while the Eifel record shifts towards an assembly dominated by grasses. It is not clear what might have caused this depletion, but since growth rates are very low after 109 ka (Fig. 4), it could be related to prior calcite precipitation (PCP). PCP is known to act as a control mechanism on seasonal variations in $\delta^{13}C$ of Han-sur-Lesse speleothems, as concluded from an elaborate cave monitoring study by Van Rampelbergh et al. (2014). However, the study by Van Rampelbergh et al. (2014) was carried out on a large, tabular-shaped stalagmite with drip water discharge rates of 300mL min-1 and growth rates of ~1mm yr-1, so caution is required when extrapolating these cave monitoring conclusions to smaller, slower growing stalagmites in a different part of the cave system. If PCP occurs at one site in the cave, it does not mean that it occurs over the entire cave (Riechelmann et al., 2011). Since no additional data on Sr and Mg is currently available for Han-9, the presence of PCP cannot be confirmed, neither rejected.

To summarize, the control on Han-9 $\delta^{13}C$ variations is the amount of biogenic CO_2 in the soil, caused by changes in the vegetation type above the cave (forest/grasses) which is directly linked to climate. Lower, depleted $\delta^{13}C$ values occur during warmer and wetter periods, when vegetation is dominated by temperate trees. Higher, enriched $\delta^{13}C$ values of speleothem calcite correspond with a higher abundance of grasses above the cave during colder/dryer climate intervals.

~~The $\delta^{13}C$ values of modern $CaCO_3$ from the Han-sur-Lesse cave average around 10‰ VPDB (Van Rampelbergh et al., 2014), 3‰ lower than the average for the Han-9. Within the time series, changes up to almost 5‰ occur (Fig. 6). Such large changes in $\delta^{13}C$ are often attributed to shifts between C3 (arboreal) and C4 (grass) vegetation, since both types of vegetation leave a different $\delta^{13}C$ imprint in the soil CO_2. This leads to more negative values for $\delta^{13}C$ in cave carbonates of a C3 dominated vegetation (-14‰ to -6‰) compared to C4 vegetation (-6‰ to -2‰) (McDermott, 2004). Indeed, pollen records for the 130-100 kyr period obtained from lake cores taken in a Maar lake in the Eifel, Germany (Fig. 1A and Fig. 7) indicate that increases of grass-like C4 pollen up to 40% of the total assembly occurred during that time period (Sirocko et al., 2005). Shifts in C3-C4 vegetation have even been observed the Vosges region, France, 300 km further south (Woillard, 1978; de Beaulieu and Reille, 1992; de Beaulieu, 2010). Based on these records and other pollen datasets for northern and central Europe (Helmens et al., 2014 and references therein) large $\delta^{13}C$ shifts in the Han-9 stalagmite could reflect changes in vegetation cover above the cave, controlled by climate changes. On the other hand, a study by Genty et al. (2003) has also shown that for temperate regions not only changes in C3-C4 vegetation determine the $\delta^{13}C$ signal, but also changes in vegetation activity. Less activity, or more specific less respiration by vegetation, results in~~

Formatted: Superscript
Formatted: Superscript
Formatted: Subscript
Formatted: Subscript
Formatted: Superscript
Formatted: Superscript
Formatted: Superscript
Formatted: Subscript
Formatted: Superscript
Formatted: Superscript
Formatted: Font: Bold

~~smaller proportions of vegetation derived CO_2 relative to atmospheric CO_2 in the soil. This isotopically heavier atmospheric CO_2 would then cause an increase $\delta^{13}C$ of the soil gas. This has also been attributed for $\delta^{13}C$ excursions on a centennial to annual scale in a Holocene speleothem from the Han-sur-Lesse cave (Van Rampelbergh et al., 2015), whereas on a seasonal scale $\delta^{13}C$ variations of speleothem calcite are attributed to Prior Calcite Precipitation (PCP) (Van Rampelbergh et al., 2014). Recent work from Schubert and Jahren (2012) has also indicated an additional control on $\delta^{13}C$ of C3 plants by photosynthetic discrimination. Recently, Wong and Breecker (2015) have shown that changes of up to ~2 ‰ over the LGM – Holocene period can be attributed to photosynthetic discrimination. This can also be taken into account, especially for time intervals were large changes in atmospheric pCO_2 are expected, such as the MIS 5e/5d transition, as evidenced by past atmospheric pCO_2 changes up to 100 ppm recorded in the Epica Dome cores in Antarctica (Petit et al., 1999).~~

5.2.3 $\delta^{18}O$

In ~~the~~ mid-latitude ~~setting of northwestern~~ Europe, ~~it is difficult to constrain the origin of speleothem $\delta^{18}O$ variations in terms of changes climate expression (i.e. temperature, precipitation), since it is known that~~ several different processes (including temperature, amount effect and ocean source)~~, with variable influence, account for this~~ influence speleothem $\delta^{18}O$ variability (McDermott, 2004). A good overview of all processes possibly influencing the speleothem $\delta^{18}O$ is given by Lachniet (2009). One of the main processes acting on both precipitation $\delta^{18}O$ and calcite $\delta^{18}O$ is temperature. Temperature fractionation on vapor condensation was estimated to be around 0.6-‰ $°C^{-1}$ (Rozanski et al., 1992) and~~whereas~~ the temperature dependent fractionation between cave drip water and speleothem calcite for ~~the~~ Han-sur-Lesse Ce~~a~~ve was calculated to be -0.2-‰ $°C^{-1}$ (Van Rampelbergh et al., 2014). ~~Combining these data gives a positive~~ The eventual relation between temperature and~~on~~ speleothem $\delta^{18}O$ will be positive, lower temperatures will thus lead to more negative speleothem $\delta^{18}O$. ~~-~~The temperature control~~is~~ has been attributed as one of the main drivers of $\delta^{18}O$ fluctuations in European speleothems (Boch et al., 2011, Wainer et al., 2013). In Han-9, this temperature control is well expressed in growth phase 2, where more positive $\delta^{13}C$ values, which reflect lower temperatures through changes in vegetation, correspond with more negative $\delta^{18}O$ (Fig. 5). This also explains the negative covariation as shown by the Pearson's correlation coefficient for growth phase 2 (Table 2). It is very likely that in this record also the amount of precipitation partly influences the $\delta^{18}O$ signal of the speleothem. In the tropics, variations in monsoonal strength are regarded as the main control on speleothem $\delta^{18}O$ via the~~is~~ amount effect (Wang et al., 2001) and changes in the amount of precipitation over time have also been considered as a driver for variations within European speleothem $\delta^{18}O$ records (Genty et al., 2003; Couchoud et al., 2009, McDermott et al., 2011). Temperature and precipitation (through the amount effect) ~~-~~controls are thus expected to contribute most to the speleothem $\delta^{18}O$ variability but as this record covers an interglacial-glacial transition, other processes acting on longer timescales (i.e., fluctuations in global ice-volume) ~~-~~should also be considered. A significant contribution is to be expected from the variations in $\delta^{18}O$ of the source, i.e. the North ~~-~~Atlantic O~~o~~cean, because of fluctuations in global ice ~~-~~volume. Waelbroeck et al. (2002) ~~has~~ estimated that during MIS 5d, average global $\delta^{18}O$ values of ocean waters were up to 0.5-‰ higher compared to MIS 5e.

~~Additionally, a study by Verheyden et al. (2014) on a Holocene speleothem from the Han-sur-Lesse cave system has shown the important effect of kinetic processes overprinting the climate $\delta^{18}O$ signal, confirmed by a strong covariation of $\delta^{18}O$ with $\delta^{13}C$ and Mg/Ca and Sr/Ca ratio's as well. Similar covariance was observed for a 500 year record from the Common Era (Van Rampelbergh et al., 2015). In case of the Han-9, covariation between~~

Formatted: Superscript

~~δ^{18}O and δ^{13}C is very low (Fig. 2A-B), so it is unlikely that kinetic processes acted on this speleothem during the LIG.~~

~~To conclude, in terms of interpreting the Han-9 δ^{13}C record, we can attribute increases up to several per mill on the glacial/interglacial and stadial/interstadial conditions to changes in vegetation type. Additional variability of the record on shorter time scales, during periods when no large changes in vegetation assembly are expected, is related to vegetation activity, in response to variating temperature and precipitation. Colder/dryer conditions would then lead to an increase in δ^{13}C. This effect is can further be enhanced by PCP occurring during drier periods. The main driver of the δ^{18}O is temperature, although changes in the amount of precipitation will act on the δ^{18}O as well.~~

5.3 Climate in the Belgian area between 125.3 and ~97 ka

5.3.1 125.3 ka: Start of speleothem growth triggered by an increase in moisture availability ~~A late onset of the Eemian?~~

~~The modeled age for the start of the Han-9 growth is 125.3 ka (Fig. 5).~~ The age model implies that Han-9 started growing at 125.3 ka (Fig. 4). Among the recent sampling missions for Belgian LIG speleothems, this is the oldest LIG sample found so far (S. Verheyden, pers. comm.). Although a flowstone from the same Han-sur-Lesse Ceave was reported to start growing at 130 +/- 10 ka (Quinif and Bastin, 1994), the accuracy of that one single alphaspectrometic dating result can be questioned. Cave systems in Belgium are known to be very sensitive recorders of glacial/interglacial changes, with speleothem deposition only during ~~optimum~~ interglacial ~~conditions~~ intervals (Quinif, 2006). ~~Strongest melting of the Greenland ice sheet and reinforced AMOC conditions were present between 131.5 and 126.5 ka.~~ Between 131.5 and 126.5 ka, the Greenland ice sheet experienced enhanced deglacial melting and also reinforced AMOC conditions were present, as identified from the MD04-2845 core from the Bay of Biscay (Sánchez Goñi et al., 2012). ~~and~~ Sspeleothem formation, however, did occur in the Alp~~ine region~~s and in southern Europe before 125.3 ka (Moseley et al., 2015; Drysdale et al., 2009). This raises the question whether or not the start of Han-9 growth is just sample specific or if it represents a real, although maybe locally confined, climate event at 125.3 ka. The SCH-5 alpine speleothem (Fig. 1A) was continuously deposited between 134.1 ± 0.7 and 115.3 ± 0.6 ka (Moseley et al., 2015). Within this record, an increase in the δ^{18}O proxy starting at 128.4 ka and lasting to 125.3 ka was identified as a warming phase. The warming phase recognized in this alpine speleothem occurs just prior to the start of the Han-9 speleothem growth, emphasizing a possible link between the warming and the start of speleothem formation in Han-sur-Lesse. In the BDInf speleothem ~~studied by Couchoud et al. (2009)~~ from southern France (Couchoud et al., 2009) (Fig. 1A), the interval between 125.3 and 123.8 ka was identified as a period with~~of~~ increased rainfall amount. A warmer/wetter period is potentially expressed in northwest European vegetation records as well, such as the Eifel m~~M~~aar record ~~from~~ (Sirocko et al., ~~(~~2005), located only 150 km from the cave site in this study. At~~The~~ 125 ka, ~~a time is marked by the~~ transition of a pollen assembly consisting mainly of pioneering *Betula* pollen with boreal *Pinus* towards an assembly significantly richer in thermophilous, broad-leaf tree pollen such as *Ulmus*, *Quercus*, *Corylus* and *Carpinus* is observed. However, the chronology of this record was not constructed independently; the start of the Eemian ~~s.s.~~ was determined by cross-correlating with the U/Th dates of the SPA-50 a~~A~~lpine speleothem record of Holzkämper et al. (2004) and set at 127 ka. The Han-9 δ^{13}C record at 125.3 ka has the most negative values for the entire 125.3-117.3 ka growth period, reaching almost -9 ‰. δ^{18}O on the other hand registers a decrease >~~–~~0.5~~–~~‰ during the first 300 years of growth (Fig. 5). The low δ^{13}C values ~~is~~ perhaps demonstrate~~s~~ that interglacial optimum conditions were already present before 125.3 ka, but that an increase in

moisture availability caused by enhanced precipitation above the cave, shown by the $\delta^{18}O$ decrease, was the factor needed to trigger growth of ~~the~~ Han-9.

5.3.2 125-120 ~~-~~ka: Eemian optimum

The isotope records of ~~the~~ Han-9 are relatively stable between 125 and ~120 ~~-~~ka (Fig. 5). The variation of $\delta^{18}O$ seems to be sub-millennial and is largely confined to between -5.7 and -6.3~~-~~‰. The long-term trend, as displayed by a fitted 7-point running average (Fig. 5~~7~~), shows lower variability between 125 and ~120 ka, especially when compared to younger growth periods of ~~the~~ Han-9 (i.e. ~~between~~ 120-117.3 ka and 112.9-106.6 ka). Similar observations are made for ~~the~~ $\delta^{13}C$: sub-millennial variability restricted between -7 and -8~~-~~‰, with the exception of a positive excursion towards -6‰ around 122 ~~-~~ka, and generally more stable than in younger~~other~~ time intervals. During 125-120 ~~-~~ka, other paleoclimate records display stable interglacial conditions, such as speleothems from the ~~Alpine region~~Alps (Meyer et al., 2008; Moseley et al., 2015) and from Italy (Drysdale et al., 2009), and other archives including ice cores (NEEM community, 2013) (Fig. 5). In marine records off the Iberian Margin, the 125-119 ka period was identified as an interval of 'sustained European warmth' ~~(Sánchez Goñi et al., 2012)~~, following a time of enhanced Greenland melting between 131.5 and 126.5 ~~-~~ka (Sánchez Goñi et al., 2012). We therefore attribute the stability of our records to the Eemian climate optimum persisting in the Belgian area as well. This is also supported by the constant growth rate (Fig. 4~~5~~) and the speleothem morphology, displaying a sequence of layered calcite which does not show any significant change over the 125-120 ka period (Fig. 2C-E).~~, with no significant change over that time (Fig. 2C-E).~~

5.3.3 120-117.3 ~~-~~ka: Inception of glacial conditions

At~~From~~ 120 ~~-~~ka ~~onwards~~, an increase in $\delta^{18}O$ of 0.5~~-~~‰ is observed (Fig. 5). This change in $\delta^{18}O$ of the speleothem corresponds with an elevated growth rate (Fig. 4) and a speleothem morphology that becomes progressively coarser, with layers that are less expressed (Fig. 2C and E).~~, supported by a decrease in stalagmite diameter.~~ No major changes in the $\delta^{13}C$ are observed. Although both the age-depth model and the speleothem morphology ~~evidence a faster~~support an increase in speleothem growth rate, possibly~~likely related~~ in response to an increase in moisture availability within the cave, there is no evidence in the Han-9 $\delta^{18}O$ record for an increase in precipitation. Due to the amount effect, enhanced precipitation would cause the $\delta^{18}O$ signal to shift towards more negative values, which is not observed in the record. The increase in growth rate and thereby accompanied faster CO_2 degassing during speleothem formation is known to act as a possible kinetic control on the speleothem $\delta^{18}O$ (Hendy, 1971; Lachniet, 2009), yet kinetic control by fast degassing would also result in positive changes of $\delta^{13}C$ (Baker et al., 1997), which is not the case here. Another possible explanation could be a temperature rise causing the elevated $\delta^{18}O$ signal, although such locally confined temperature increase seems unlikely, because no other records (pollen, sea surface temperature~~SST~~) support~~s~~ this hypothesis. Most likely, this increase in $\delta^{18}O$ is not related to any local climate effects but reflects a more regional~~ly~~ signal, which could be the increase of the source $\delta^{18}O$ of the North Atlantic O~~o~~cean, since a rise of 0.5~~-~~‰ is in good agreement with estimations of the source $\delta^{18}O$ variability over the MIS 5e/5d transition from Waelbroeck et al. (2002). As a matter of fact, a study by Hearty et al. (2007) combining ~~Last Interglacial~~last interglacial sea-level evolution at 15 sites around the world shows a rapid descent towards an MIS 5d low stand at 119 ± 2 ~~-~~ka. This also favors the hypothesis that the speleothem $\delta^{18}O$ between 120 and 117.3 ka reflects changing ocean source due to ice build-up.

A severe change in the $\delta^{13}C$ is not observed until 117.5 ka, where a sudden increase towards -4 ‰ occurs (Fig. 5). This 5 ‰ change takes place within 200 years and happens just before the first hiatus in this speleothem, suggesting that the cessation in speleothem growth is indeed caused by a climate event. The increase in $\delta^{13}C$ here is believed to reflect changes in vegetation, such as an increase in grasses resulting in lower vegetation activity, linked to a changing (drying and/or cooling) climate. The age of this event, 117.3 ka, stands out in other studies as well. First of all, in the NGRIP $\delta^{18}O$ record it falls within what is identified as Greenland Stadial 26 (NGRIP Members, 2004). Although the signature of this GS may not be as clear as the younger GS 25 or 24, it corresponds with the overall decreasing trend observed in the ice $\delta^{18}O$, and is also recognized in the more recent NEEM ice core (NEEM community, 2013). The global character of this climate event around 117.3 ka is evidenced by similar changes in the North Atlantic Ocean. A high-resolution study by Galaasen et al. (2014) has found perturbations of the $\delta^{13}C$ of benthic foraminifera in marine sediment cores, interpreted as a sharp decrease in North Atlantic Deep Water (NADW) formation at 116.8 ka, in contrast with the high NADW formation observed during the MIS 5e. Such reductions in NADW led to changes in AMOC, resulting in a reduced ocean heat transport and eventually cooling of the climate. This hypothesis is further evidenced by lower sea surface temperatures, shown by an increase in planktonic foram $\delta^{18}O$, and the presence of IRD in marine core MD03-2664 at that time (Irvali et al., 2012) (Fig. 5). The lower resolution in the sea surface temperature record of core MD04-2548 retrieved from the Bay of Biscay (Fig. 1A) could explain its absence in this archive (Fig. 5). Other accurately dated European speleothem records mark a similar climate deterioration around the same time. Perhaps the most obvious example is the study from Meyer et al. (2008), where a 3 to 4 ‰ drop in $\delta^{18}O$ of four different flowstones from the Entrische Kirche cave (Fig. 1A) is observed between 119 and 118 ka (Fig. 5). This large drop in speleothem $\delta^{18}O$ is believed to be caused by a severe cooling, and was defined as the glacial inception at the cave site. Furthermore, a subtle depletion occurs in the HÖL-10 stalagmite (Fig. 5) and was correlated to the $\delta^{18}O$ drop from Entrische Kirche (Moseley et al., 2015). Closer to the Han-sur-Lesse Cave, a similar event was also observed in the Eifel Maar record. There it was identified as the 'LEAP' or the Late Eemian Aridity Pulse and defined by an increase in varve thickness, loess and charcoal content together with a higher abundance of grass pollen within the assembly (Sirocko et al., 2005), which would explain the increase in $\delta^{13}C$ of the Han-9. Yet, the timing of the LEAP predates the Han-9 event by ~1 ka. Nevertheless, we suggest that both records registered the same event and that the offset in chronology can be caused by the tuning of the Eifel record or the uncertainty of the Han-9 age-depth model at 117.3 ka.

5.3.4 117.3-97 ka: Stadial/Interstadial changes in the Early Weichselian

After the first hiatus, growth starts again at 112.9 ka. The LEAP event in the Eifel maar only lasts 468 years (Sirocko et al., 2005), yet speleothem growth does not recover immediately after the LEAP event. A similar observation was made for the start of speleothem growth at 125.3 ka: optimum conditions were already present before Han-9 started growing. From this delayed growth, it appears that climate conditions need to be more favorable (warmer/wetter) to initiate growth than to sustain growth. During the second growth phase of the Han-9 stalagmite (112.9-106.6 ka), interesting differences occur compared to the earlier formed part of the speleothem. First of all, the variation of both $\delta^{18}O$ and $\delta^{13}C$ is much larger (Fig. 5). Secondly, changes in stalagmite morphology appear, with alternations between dense, darker calcite and more white, coarser calcite (Fig. 2C-E). The $\delta^{13}C$ curve of the Han-9 shows a long-term increasing trend of increase until a maximum of -4 ‰ is reached at 110 ka. Superimposed on this trend, (sub-)millennial variability ranging between 2 and 3 ‰ is present. In contrast, within the $\delta^{18}O$ record a long-term trend is not as obvious, although a minimum of -6.8 ‰ is

reached between 111 and 110 -ka. ~~Both minima in stable isotope proxies~~The maximum in $\delta^{13}C$ and the minimum in $\delta^{18}O$ -correspond well with the timing of GS 25 (110.6~~11~~-108.3 ~~9~~-ka, Rasmussen et al., 2014) observed in the NGRIP record (plotted on the GICC05modelext timescale), implying that the stable isotopes of Han-9 reflect the temperature decrease of the stadial, which is likely since higher $\delta^{13}C$ is linked to a less active vegetation cover during colder periods (~~or more C4 vegetation~~i.e. more grasses) and lower $\delta^{18}O$ is caused by lower temperatures. The timing in the Han-9 record is also in agreement with the GS 25 registered in the NALPS record, which is believed to be dominantly temperature dependent (Boch et al., 2011). The summer s~~S~~ea s~~S~~urface t~~T~~emperature reconstructions for marine core MD04-2845 show a distinct decrease of ~10°C ~~(Sánchez Goñi et al., 2012)~~ at the same time (Sánchez Goñi et al., 2012). Between 112.9 and 111 ka, ~~T~~the variability of $\delta^{13}C$ and $\delta^{18}O$ in~~ the~~ Han-9, predating GS 25, ~~(112.9-111 ka)~~ has an inverse relationship suggesting that $\delta^{18}O$~~it~~ is mainly temperature controlled. The ice build-up effect, displayed by the increase in $\delta^{18}O$ between 120 and 117.3 ka, is cancelled out by the effect of lower temperature, causing a decrease in speleothem $\delta^{18}O$. It ~~thus~~ also appears that for a general cooler climate state, the amplitude of variability tends to increase as well, compared to a more stable Eemian optimum (125-120 ~~0~~-ka). The timing of the second hiatus (106.6-103 -ka) is similar to that of the occurrence of GS 24 in the NGRIP record~~curve~~ and is also registered in the NALPS dataset from Boch et al. (2011). However, if the hiatus has any affinity with ~~the~~ GS 24, this raises the question why speleothem growth stopped during GS 24 and continued during~~ the~~ GS 25~~ period~~. A plausible explanation could be that growth never fully recovered from the GS 25, and that less favorable conditions (cooler/dryer) during the GS 24 interval were sufficient to cease growth. This assumption is grounded by decreased growth rate from 110 -ka onwards (Fig. 4~~5~~). In the Eifel m~~M~~aar core, significant changes in vegetation occur from ~112 -ka, with nearly all pollen from broadleaf trees disappearing and the transition towards a pollen assembly dominated by coniferous trees and grasses (Fig. 5~~7~~). Also, the time periods 110-108.5 -ka and 106-104.5 -ka are characterized by a significant increase in loess composition~~content~~ and varve thickness, indicative for dryer conditions in that area and corresponding with the GS 25 and GS 24 intervals (Sirocko et al., 2005). ~~In the third growth phase of the Han-9 (103.6 – ~97 ka), $\delta^{13}C$ reaches its minimum, with a range between -8.5 and -10.5, which is far lower than the average during the Eemian growth. This is remarkable, as pollen tend towards an assembly richer in grasses (Sirocko et al., 2005). However, it is difficult to make any further conclusions on this, as the age model is only poorly constrained below 103.6 ka (Fig. 5).~~

6. Conclusions

This study highlights the potential of Belgian speleothem proxies (i.e. growth, morphology and stable isotopes) as recorders of regional and local climate change over the Eemian and early ~~Early~~ Weichselian in northwestern Europe. The start of speleothem growth occurs at 125.3 -ka. At that time however, nearly all of the European continental records are already within the Eemian climate optimum state. The $\delta^{18}O$ record suggests that the eventual trigger starting speleothem growth was most likely moisture availability, linked to an increase in (local) precipitation at that time. Optimum Eemian climate conditions recorded in~~ the~~ Han-9 occurred between 125.3 and 120 -ka, and the stable isotopes and speleothem morphology indicate a relatively stable climate state. The ~~F~~first signs of regional changing climate are observed in the $\delta^{18}O$ proxy from 120 -ka onwards, and are linked to a changing ocean source $\delta^{18}O$, caused by increasing ice volume. The end of the Eemian (and start of the ~~Early~~ early Weichselian) in~~ the~~ Han-9, at 117.3 -ka, is preceded by a drastic change in vegetation activity and/or assembly that took place within 200 years, triggered by a decrease in moisture availability linked to a drying climate. This eventually led to cessation of speleothem growth. This event appears to have a broad regional signature, as it is registered in other European records as well. However, pollen records imply that temperate

vegetation seems to persist several millennia after 117.3 ka (de Beaulieu and Reille, 1992; Sirocko et al., 2005), ~~giving~~resulting in a~~to~~ longer duration~~s~~ of the Eemian ~~as defined~~ in other records (Tzedakis et al., 2003). In addition, Han-9 also registered three ~~Greenland s~~Stadials occurring during the e~~E~~arly -Weichselian. ~~The start of~~ During GS 26, at 117.3 ka, ~~is simultaneous with the~~ the end of the Eemian in Han-9 ~~at 117.3 ka~~occurs. ~~,~~The GS 25 equivalent occurs between 110.5 and 108.5 ka~~–~~ as deduced from the stable isotope proxies and GS 24 is represented by a hiatus in Han-9 that starts at 106.6 ka. These chronologies are consistent with other European speleothem records. ~~GS 25 is characterized by changes in vegetation (activity) caused by decrease in temperature and precipitation, whereas GS 24 is marked by a stop in speleothem growth.~~ For the e~~E~~arly -Weichselian, local climate appears to be more sensitive during the early glacial conditions as the amplitude and frequency of ~~variability~~ isotopic shifts tends to increase significant compared to the Eemian.

Data availability. Stable isotope time-series for the first two growth phases are available online at NOAA paleoclimate database.

Acknowledgements. We thank the Domaine des Grottes de Han for allowing us to sample the stalagmite and to carry out other fieldwork. S. Vansteenberge thanks D. Verstraeten for the assistance with the stable isotope measurements. Ph. Claeys thanks the Hercules Foundation for upgrade of the Stable Isotope laboratory at VUB, and the VUB Strategic Research funding.

Table 1

Sample Number	DFT (mm)	^{238}U (ppb)	^{232}Th (ppt)	$^{230}Th / ^{232}Th$ (atomic x10^{-6})	$\delta^{234}U^{*}$ (measured)	$^{230}Th / ^{238}U$ (activity)	^{230}Th Age (yr) (uncorrected)	^{230}Th Age (yr) (corrected)	$\delta^{234}U_{Initial}^{**}$ (corrected)	^{230}Th Age (yr BP)*** (corrected)
DAT-10	668	531,5 ±0,6	1693 ±34	6077 ±122	622,5 ±1,5	1,1739 ±0,0016	124854 ±363	124805 ±364	885 ±2	124740 ±364
DAT-1	**639**	**475,3 ±0,4**	**6419 ±128**	**1417 ±29**	**606 ±3**	**1,1608 ±0,0027**	**124781 ±653**	**124569 ±669**	**862 ±4**	**124506 ±669**
DAT-11	614,6	227,6 ±0,2	413 ±8	11096 ±223	704,0 ±1,6	1,2220 ±0,0013	122075 ±304	122049 ±305	993 ±2	121984 ±305
DAT-12	581,5	289,7 ±0,2	1597 ±32	3563 ±71	675,2 ±1,5	1,1911 ±0,0014	120625 ±304	120542 ±310	949 ±2	120477 ±310
DAT-2	**554**	**370,5 ±0,3**	**213 ±4**	**33652 ±692**	**661 ±3**	**1,1759 ±0,0029**	**119934 ±589**	**119925 ±589**	**927 ±4**	**119862 ±589**
DAT-13	484,2	390,1 ±0,4	1420 ±28	5246 ±105	637,7 ±1,6	1,1583 ±0,0015	119971 ±331	119915 ±333	895 ±2	119850 ±333
DAT-14	426	337,7 ±0,3	243 ±5	26740 ±539	656,3 ±1,5	1,1679 ±0,0013	119179 ±289	119168 ±289	919 ±2	119103 ±289
DAT-3	**397**	**373,4 ±0,3**	**681 ±14**	**10480 ±211**	**650 ±2**	**1,1596 ±0,0027**	**118564 ±539**	**118536 ±539**	**908 ±3**	**118473 ±539**
DAT-15	356	636,0 ±0,7	1406 ±28	8600 ±172	648,9 ±1,5	1,1533 ±0,0014	117661 ±306	117627 ±307	904 ±2	117562 ±307
DAT-4	**311**	**226,6 ±0,3**	**1735 ±35**	**2526 ±51**	**667 ±3**	**1,1727 ±0,0036**	**118596 ±727**	**118481 ±731**	**932 ±5**	**118418 ±731**
DAT-5	**297**	**396,8 ±0,4**	**563 ±11**	**13324 ±269**	**677 ±2**	**1,1456 ±0,0027**	**112964 ±512**	**112942 ±512**	**931 ±4**	**112879 ±512**
DAT-17	271	213,5 ±0,1	1647 ±33	2460 ±49	692,3 ±1,4	1,1511 ±0,0011	112045 ±237	111930 ±251	949 ±2	111865 ±251
DAT-18	238,5	239,0 ±0,2	208 ±4	21967 ±446	709,8 ±1,6	1,1594 ±0,0012	111337 ±254	111324 ±254	972 ±2	111259 ±254
DAT-6	**214**	**216,2 ±0,3**	**939 ±19**	**4315 ±87**	**691 ±3**	**1,1365 ±0,0035**	**109887 ±637**	**109822 ±638**	**943 ±4**	**109759 ±638**
DAT-16	201	158,8 ±0,1	386 ±8	7695 ±155	680,1 ±1,5	1,1334 ±0,0012	110663 ±245	110627 ±246	929 ±2	110562 ±246
DAT-19	179,5	179,8 ±0,1	3158 ±63	1064 ±21	711,7 ±1,5	1,1341 ±0,0011	107303 ±223	107042 ±289	963 ±2	106977 ±289
DAT-7	**171**	**187,0 ±0,2**	**1051 ±21**	**3255 ±66**	**712 ±4**	**1,1089 ±0,0037**	**103615 ±671**	**103531 ±673**	**953 ±6**	**103468 ±673**
DAT-20	154	204,3 ±0,2	2749 ±55	1339 ±27	727,0 ±1,5	1,0929 ±0,0011	99868 ±215	99668 ±257	963 ±2	99603 ±257
DAT-21	125,7	159,7 ±0,1	1709 ±34	1673 ±34	744,0 ±1,6	1,0861 ±0,0011	97373 ±206	97215 ±234	979 ±2	97150 ±234
DAT-8	**98,7**	**149,3 ±0,2**	**759 ±15**	**3593 ±73**	**737 ±4**	**1,1070 ±0,0039**	**100847 ±664**	**100772 ±666**	**980 ±6**	**100709 ±666**
DAT-22	56	196,9 ±0,1	978 ±20	3503 ±70	694,6 ±1,5	1,0554 ±0,0011	97680 ±206	97604 ±212	915 ±2	97539 ±212
DAT-23	34	234,0 ±0,2	359 ±7	11228 ±226	668,5 ±1,6	1,0444 ±0,0013	98598 ±236	98574 ±237	883 ±2	98509 ±237
DAT-9	**15,2**	**240,4 ±0,2**	**531 ±11**	**7898 ±161**	**677 ±3**	**1,0581 ±0,0039**	**99784 ±634**	**99750 ±634**	**897 ±4**	**99687 ±634**

U decay constants: $\lambda_{238} = 1.55125x10^{-10}$ (Jaffey et al., 1971) and $\lambda_{234} = 2.82206x10^{-6}$ (Cheng et al., 2013). Th decay constant: $\lambda_{230} = 9.1705x10^{-6}$ (Cheng et al., 2013).
*$\delta^{234}U = ([^{234}U/^{238}U]_{activity} - 1)x1000$. ** $\delta^{234}U_{initial}$ was calculated based on ^{230}Th age (T), i.e., $\delta^{234}U_{initial} = \delta^{234}U_{measured} \times e^{\lambda 234 \times T}$.
Corrected ^{230}Th ages assume the initial $^{230}Th/^{232}Th$ atomic ratio of 4.4 ±2.2 x10^{-6}. Those are the values for a material at secular equilibrium, with the bulk earth $^{232}Th/^{238}U$ value of 3.8. The errors are arbitrarily assumed to be 50%.
***B.P. stands for "Before Present" where the "Present" is defined as the year 1950 A.D.

585

Table 1. U/Th measurements of the Han-9 ~~s~~Stalagmite (University of Minnesota). Samples are arranged in stratigraphic order and those in bold indicate results acquired in 2013.

Table 2

	ρ	# measurements
Growth Phase 1	0,024	599
Growth Phase 2	-0,467	235
Growth Phase 3	0,461	284
Total	-0,197	1118

Table ~~2~~1: Pearson's coefficient of correlation (ρ) calculated for the three growth phases and for the total record.

Formatted: Font: 10 pt

Formatted: Font: 10 pt

	$\delta^{13}C$	$\delta^{18}O$
RC1	-8,19	-5,73
RC2	-8,20	-6,25
RC3	-7,80	-6,48

590

Table ~~3~~2: $\delta^{13}C$ and $\delta^{18}O$ analysis of three recent calcite samples (RC1 to RC3) from the *Réseau Renversé*.

Formatted: Font: 10 pt

Formatted: Font: 10 pt

Figure 1

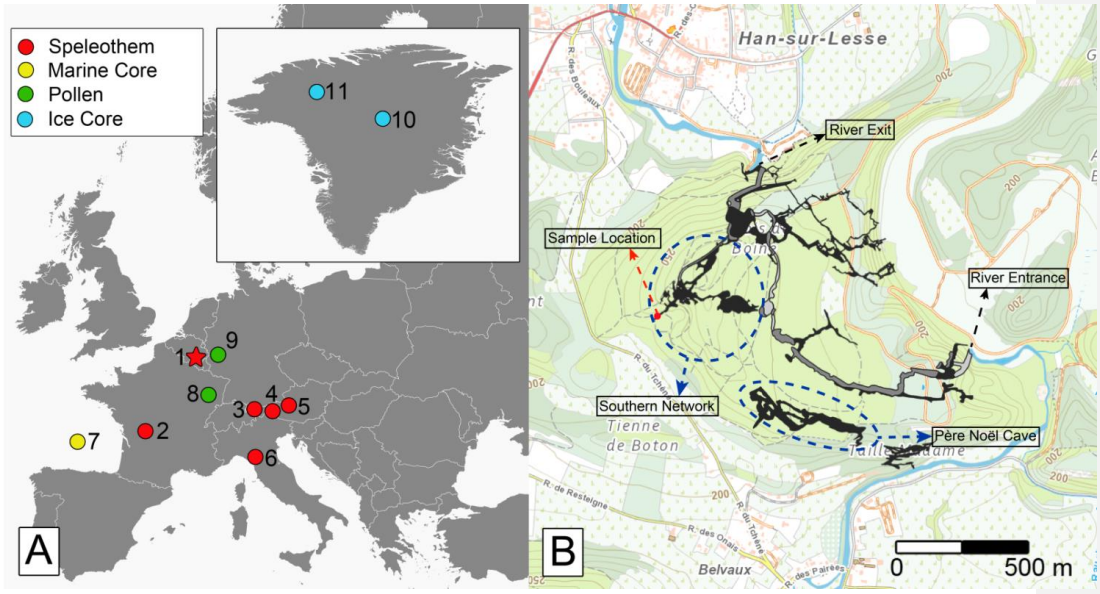

Figure 1 A) Location of the Han-sur-Lesse Cave site (Red Star) and other records mentioned in this study 1) Han-sur-Lesse; 2) Bourgeois-Delaunay Cave (Couchoud et al., 2009); 3) Hölloch Cave (Moseley et al., 2015); 4) Spannagel Cave (Hölzkamper et al., 2004); 5) Entrische Kirche Cave (Meyer et al., 2008); 6) Corchia Cave (Drysdale et al., 2009); 7) MD04-2548 (Sanchez-Goñi et al., 2012); 8) La Grande Pile (Woillard, 1978); 9) Eifel Maar (Sirocko et al., 2005); 10) NGRIP (NGRIP Members, 2004); ~~and~~ 11) NEEM (NEEM community, 2013) and 12) MD03-2664 (Irvali et al., 2012). **B~~b~~)** Topographic map of the study area (source: NGI Belgium). The Han-sur-Lesse Cave system is plotted in black. The sampling site of ~~the~~ Han-9 is marked by the yellow~~red~~ dot, the purple dot represents the location of cave monitoring by Van Rampelbergh et al. (2014). The ~~Southern Network~~*Réseau Sud* and the *Réseau Renversé* are shown by the red and orange box. ~~Père Noël cave are indicated with the dashed circles.~~ For further explanation, see text. ~~-~~Figure adapted from Quinif (2006).

Formatted: Font: Not Italic

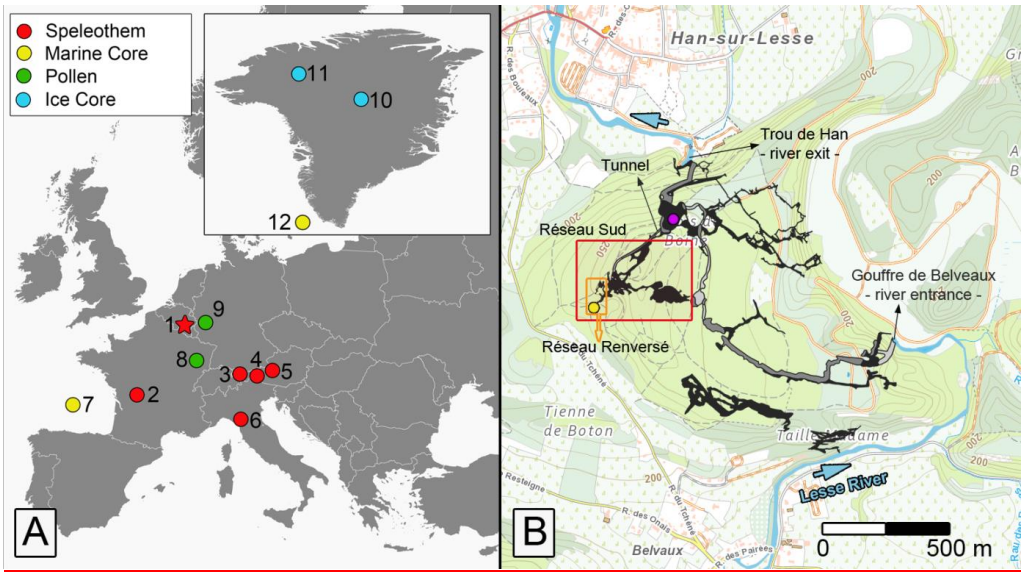

595

600

605

~~**Figure 2**~~

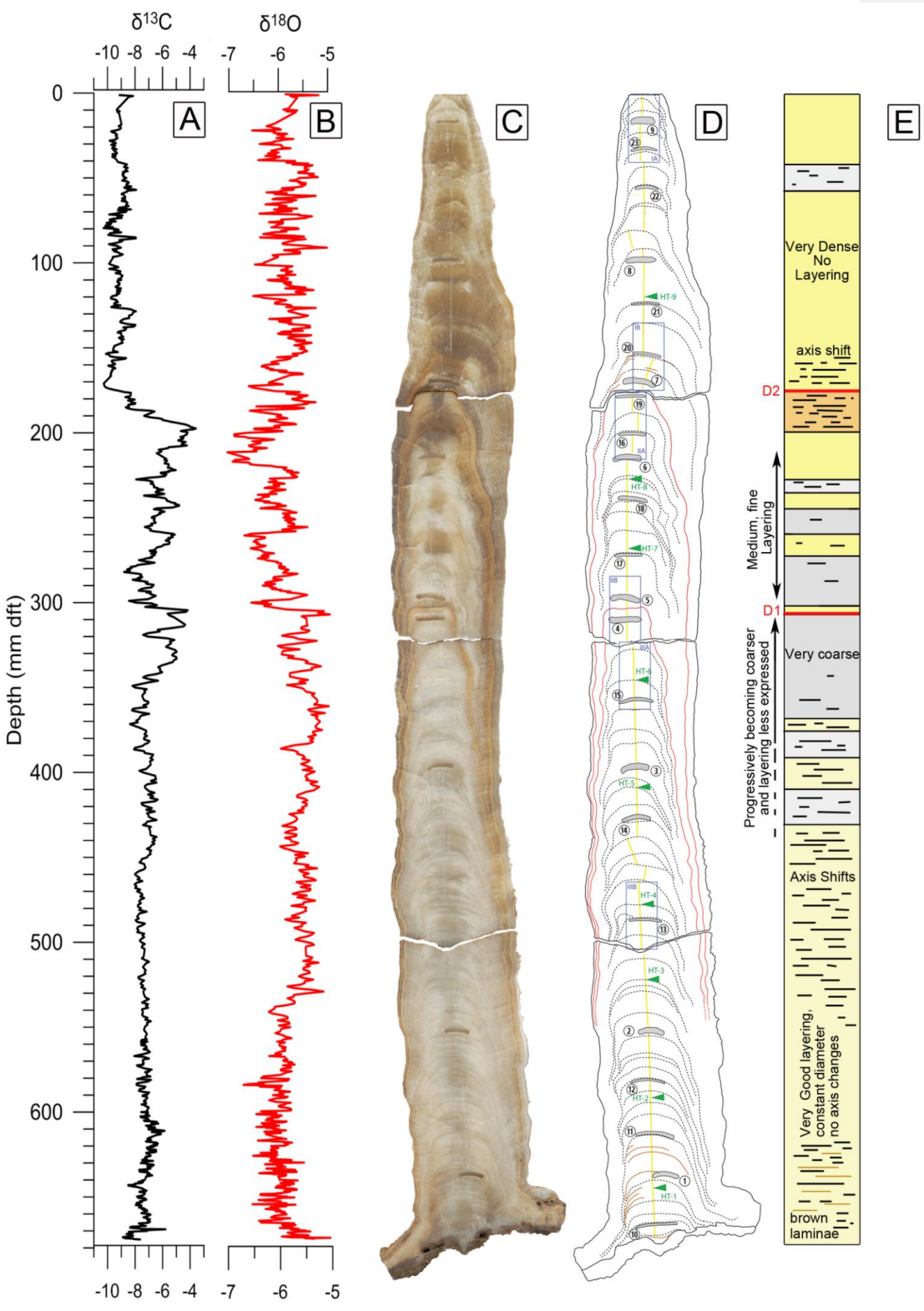
δ13C
δ18O
-10 -8 -6 -4
-7 -6 -5
A
B
C
D
E
Depth (mm dft)
0
100
200
300
400
500
600
Very Dense
No
Layering
axis shift
D2
Medium, fine
Layering
D1
Very coarse
Progressively becoming coarser
and layering less expressed
Axis Shifts
Very Good layering,
constant diameter
no axis changes
brown
laminae

610

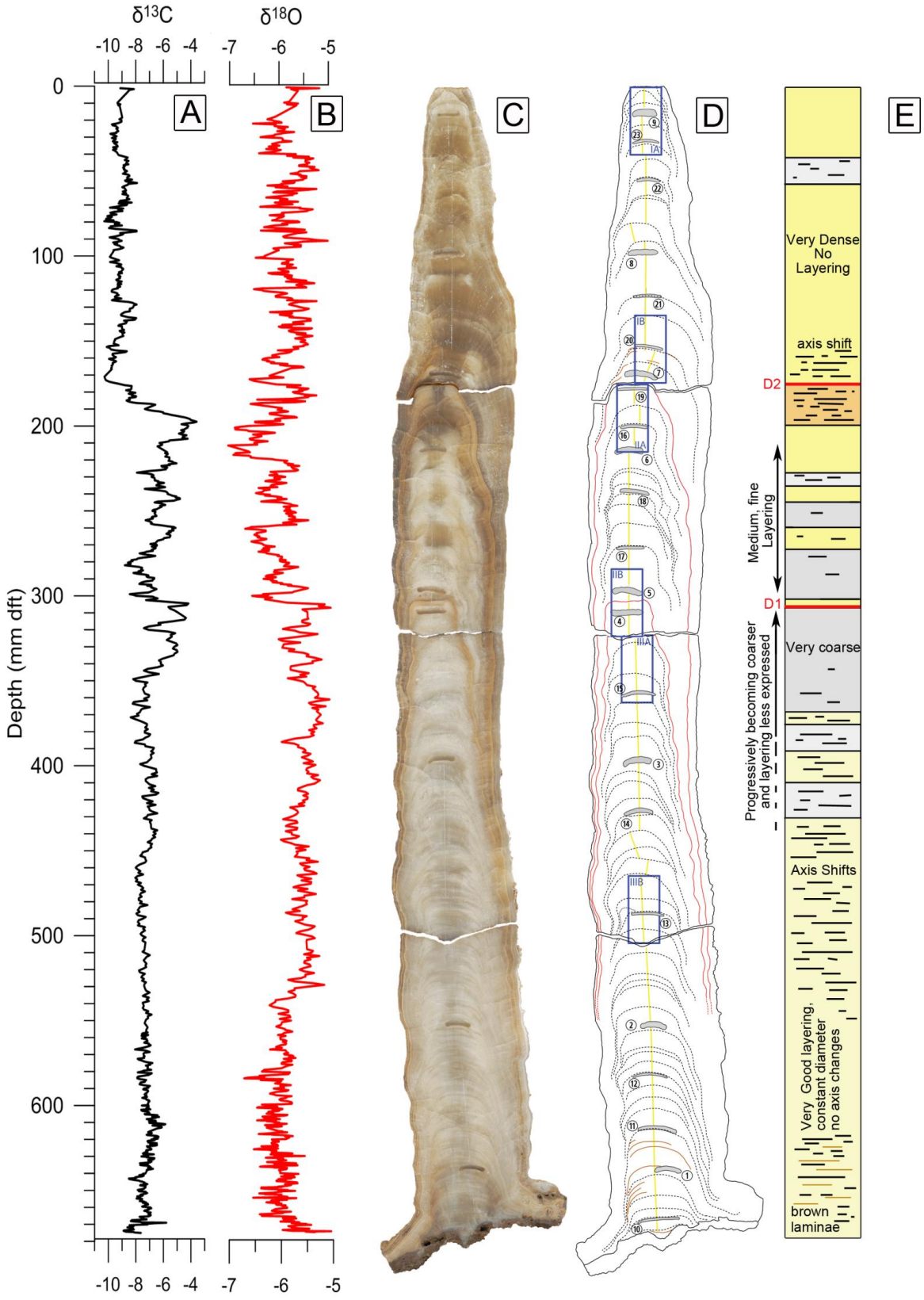
δ13C
δ18O
-10 -8 -6 -4
-7 -6 -5
A
B
C
D
E
Depth (mm dft)
0
100
200
300
400
500
600
IA
IB
IIA
IIB
IIIA
IIIB
Very Dense
No
Layering
axis shift
D2
Medium, fine
Layering
D1
Very coarse
Progressively becoming coarser
and layering less expressed
Axis Shifts
Very Good layering,
constant diameter
no axis changes
brown
laminae

Figure 2: Descriptive image of Han-9 **A)** $\delta^{13}C$ plotted against distance from top in mm; **B)** ~~similar but now for~~ $\delta^{18}O$ plotted against distance from top in mm; **C)** High-resolution scan of the polished slabs; **D)** Interpretation of the internal structure of the speleothem. Dashed lines = distinctive layers; Red lines = growth discontinuities; Grey areas = dating samples, numbers refer to the samples in Table 1; Yellow line = central axis (sample axis); Blue boxes = thin section locations~~; Green triangles = Hendy test locations~~; Brown lines = detrital material. **E)** Stratigraphic log: colors indicate the presence of dense calcite (yellow) or coarse calcite (grey), more intense color = denser/coarser compared to lighter colored parts. The visual expression of layering is indicated with the dashes in the log. Further description of the log can be found in the figure and text.

Figure 3

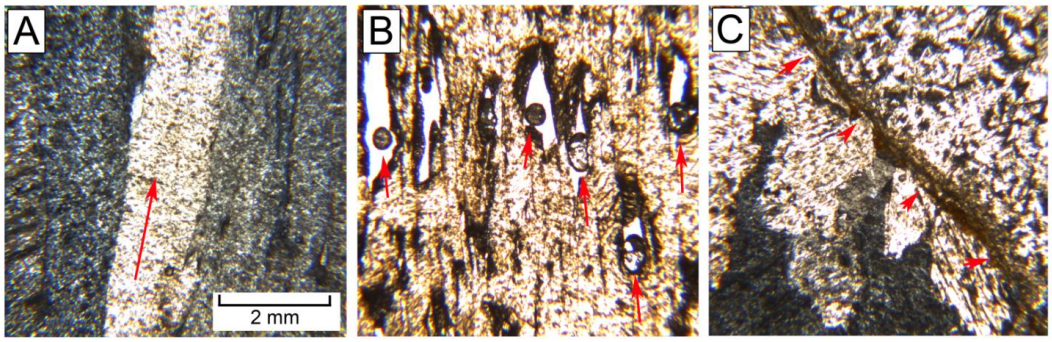

Figure 3: Thin section images of ~~the~~ Han-9. For locations, see Fig. 2D. All pictures are taken with crossed polarized light, have the same scale and speleothem growth direction is upwards **A)** Thin section IIIB: (Elongated) columnar calcite fabric. **B)** IIIA: Open columnar fabric, with fluid inclusions in the open voids **C)** IIA: Discontinuity D2 is characterized by presence of brown detrital material. Also note the different fabric underneath the hiatus.

~~**Figure 4**~~

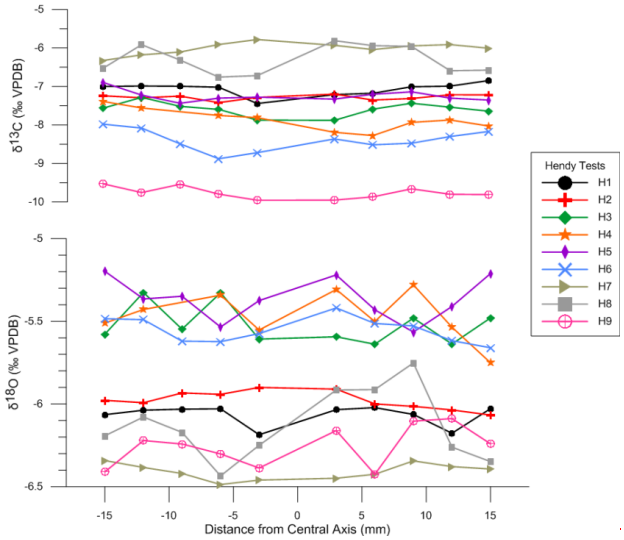

Figure 4: Results of the 9 Hendy tests carried out on the Han-9 stalagmite. Location of the tests can be found in Fig. 2D.

~~Figure~~Figure 4

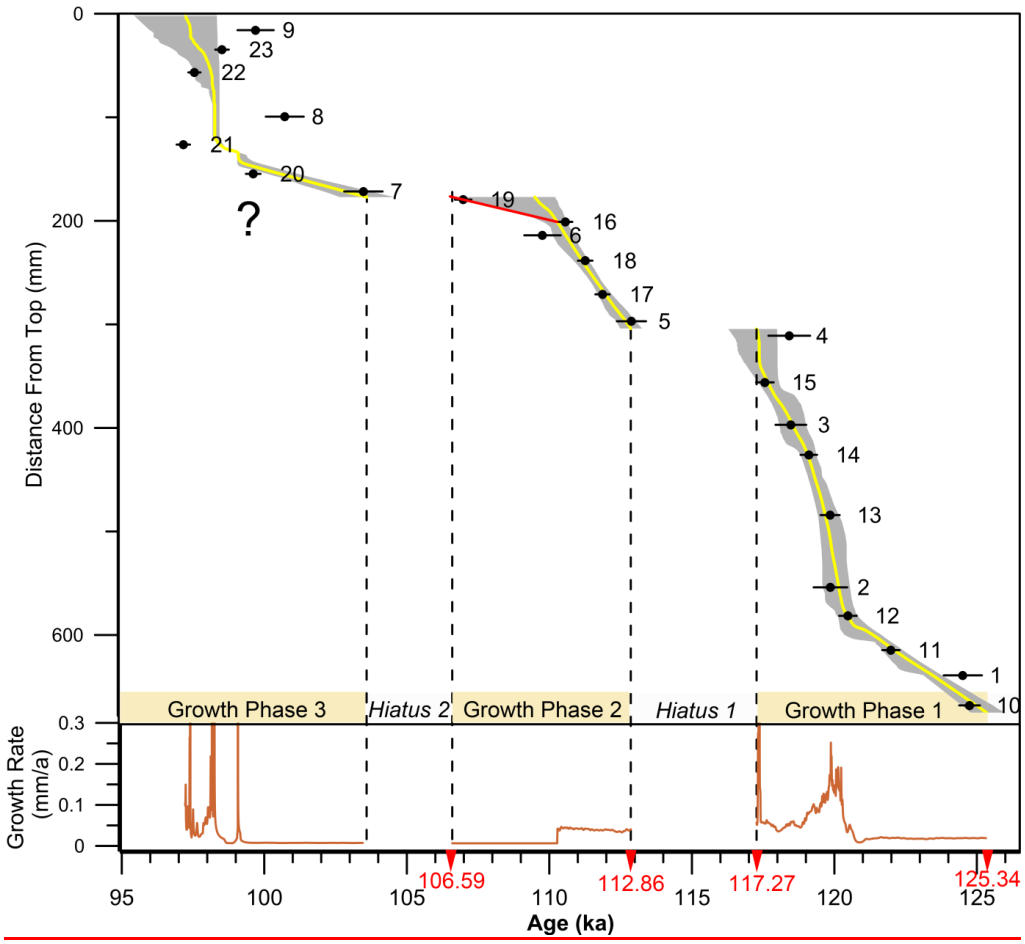

Figure 4: Han-9 age-depth model constructed with the StalAge algorithm (Scholz and Hoffmann, 2011). The actual age-depth model is represented by the yellow line, the grey area marks the error (2σ). Numbers represent the sample labels (Table 1 in original manuscript). The brown curve displays the growth rate. Numbers in red indicate important dates and are discussed in the text.

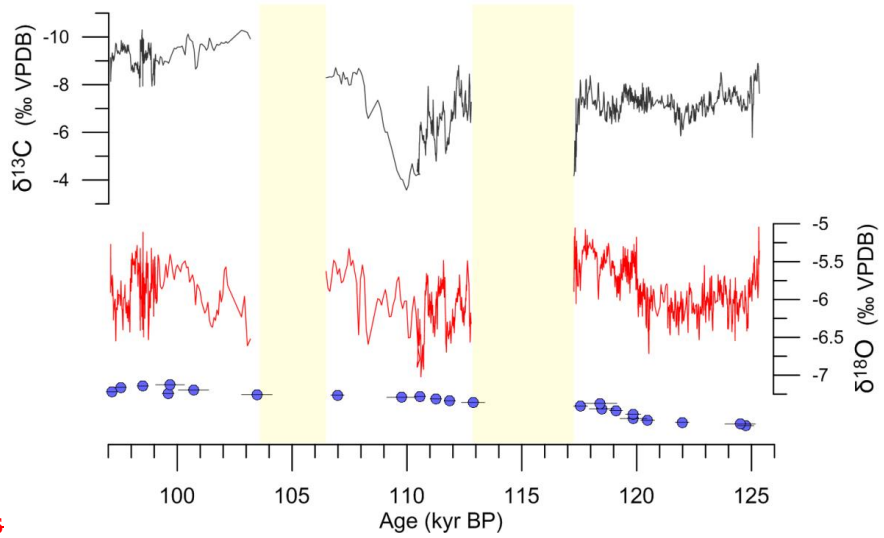

~~Figure 6~~

Figure 6: $\delta^{13}C$ (black, inverted axis) and $\delta^{18}O$ (red) time-series of the Han-9. In blue are the individual U/Th dates (see Table 1). Yellow bands mark the two~~2~~ hiatuses present in the speleothem.

Figure 5

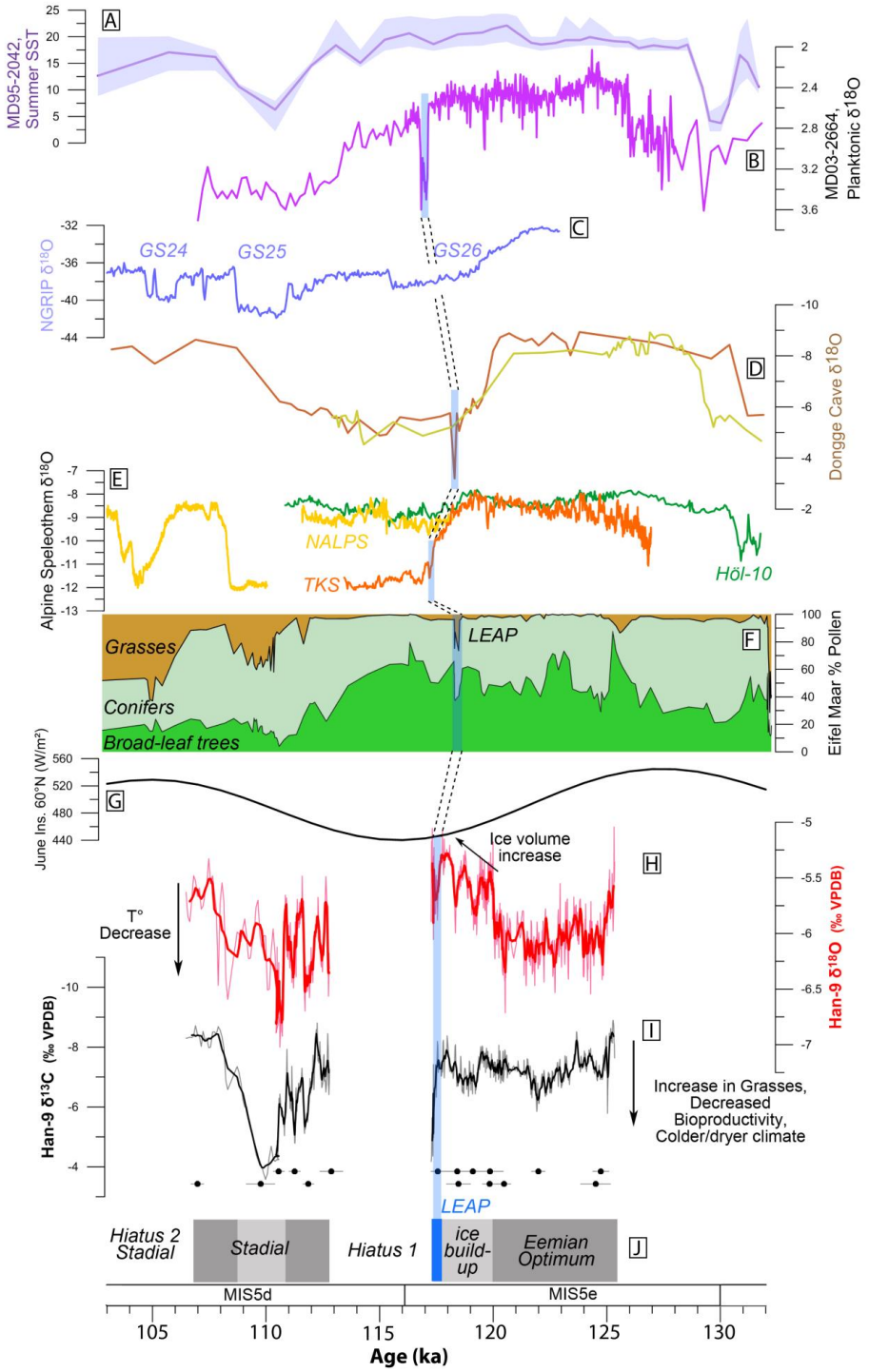
A
MD95-2042, Summer SST
B
MD03-2664, Planktonic δ18O
C
NGRIP δ18O
GS24
GS25
GS26
D
Dongge Cave δ18O
E
Alpine Speleothem δ18O
NALPS
TKS
Höl-10
F
Grasses
Conifers
Broad-leaf trees
LEAP
Eifel Maar % Pollen
G
June Ins. 60°N (W/m²)
Ice volume increase
H
Han-9 δ18O (‰ VPDB)
T° Decrease
I
Han-9 δ13C (‰ VPDB)
Increase in Grasses, Decreased Bioproductivity, Colder/dryer climate
LEAP
Hiatus 2 Stadial
Stadial
Hiatus 1
ice build-up
Eemian Optimum
J
MIS5d
MIS5e
105
110
115
120
125
130
Age (ka)

Figure 5: Comparison of Han-9 stalagmite with other records. The shaded blue area marks the occurrence of the Late Eemian Aridity Pulse (LEAP) in the Eifel record and its equivalent in other records. **A)** Sea Surface Temperature (SST) reconstruction from marine core MD04-2845 (Sanchez-Goñi et al., 2012); **B)** Planktonic $\delta^{18}O$ from marine core MD03-2664 (Irvali et al., 2012); **C)** NGRIP $\delta^{18}O$ record with indication of Greenland Stadial intervals (NGRIP members, 2004); **D)** Asian monsoon reconstructions from Dongge Cave (D3 & D4 stalagmites; Yuan et al., 2004); **E)** Alpine speleothem $\delta^{18}O$ (TKS: Meyer et al., 2008; NALPS: Boch et al., 2011; HöL-10: Moseley et al., 2015)**; F)** Eifel Maar pollen assembly (Sirocko et al., 2005); **G)** June insolation for 60°N (Berger and Loutre, 1991); **H)** & **I)** Han-9 stable isotope record with a 7-point moving average and U/Th dates; **J)** Paleoclimate interpretation of Han-9.

References

Baker, A., Ito, E., Smart, P. L., and McEwan, R. F.: Elevated and variable values of C-13 in speleothems in a British cave system, Chemical Geology, 136, 263-270, 10.1016/s0009-2541(96)00129-5, 1997.

Bar-Matthews, M., Ayalon, A., Kaufman, A., and Wasserburg, G. J.: The Eastern Mediterranean paleoclimate as a reflection of regional events: Soreq cave, Israel, Earth and Planetary Science Letters, 166, 85-95, http://dx.doi.org/10.1016/S0012-821X(98)00275-1, 1999.

Barker, S., Chen, J., Gong, X., Jonkers, L., Knorr, G., and Thornalley, D.: Icebergs not the trigger for North Atlantic cold events, Nature, 520, 333-336, 2015.

Bastin, B., and Gewelt, M.: Analyse pollinique et datation 14C de concrétions stalagmitiques Holocènes: apportes complémentaires des deux méthodes, Géographie physique et Quaternaire, 40, 185-196, 1986.

Berger, A., and Loutre, M. F.: An Exceptionally Long Interglacial Ahead?, Science, 297, 1287-1288, 10.1126/science.1076120, 2002.

Boch, R., Cheng, H., Spotl, C., Edwards, R. L., Wang, X., and Hauselmann, P.: NALPS: a precisely dated European climate record 120-60 ka, Climate of the Past, 7, 1247-1259, 10.5194/cp-7-1247-2011, 2011.

Bond, G., Broecker, W., Johnsen, S., McManus, J., Labeyrie, L., Jouzel, J., and Bonani, G.: Correlations between climate records from North-Atlantic sediments and Greenlan Ice, Nature, 365, 143-147, 10.1038/365143a0, 1993.

Bond, G. C.: Climate and the conveyor, Nature, 377, 383-384, 1995.

Bonniver, I.: Hydrogéologie du Massif de Boine, in: EcoKarst, 3, La Hulpe, 1-4, 2010.

Bonniver, I.: Etude Hyrogeologique et dimmensionnement par modelisation du “systeme-tracage” du reseau karstique the Han-sur-Lesse (Massif de Boine, Belgique), in: Géologie, FUNDP Namur, Namur, 93-97, 2011.

~~Bosch, J. H. A., and Cleveringa, P. M., T.: The Eemian stage in the Netherlands: history, character and new research Netherlands Journal of Geosciences, 79, 135-145, 2000.~~

Broecker, W. S., Peteet, D. M., and Rind, D.: Does the ocean-atmosphere system have more than one stable mode of operation?, Nature, 315, 21-26, 1985.

Couchoud, I., Genty, D., Hoffmann, D., Drysdale, R., and Blamart, D.: Millennial-scale climate variability during the Last Interglacial recorded in a speleothem from south-western France, Quaternary Science Reviews, 28, 3263-3274, 10.1016/j.quascirev.2009.08.014, 2009.

Cheng, H., Edwards, R. L., Chuan-Chou, S., Polyak, V. J., Asmerom, Y., Woodhead, J., Hellstrom, J., Yongjin, W., Xinggong, K., Spotl, C., Xianfeng, W., and Alexander, E. C., Jr.: Improvements in 230Th dating, 230Th and 234U half-life values, and U-Th isotopic measurements by multi-collector inductively coupled plasma mass spectrometry, Earth and Planetary Science Letters, 371-372, 82-91, 10.1016/j.epsl.2013.04.006, 2013.

Dansgaard, W., Johnsen, S. J., Clausen, H. B., Dahl-Jensen, D., Gundestrup, N. S., Hammer, C. U., Hvidberg, C. S., Steffensen, J. P., Sveinbjornsdottir, A. E., Jouzel, J., and Bond, G.: Evidence for general instability of past

Formatted: Dutch (Belgium)

climate from a 250-kyr ice-core record, Nature, 364, 218-220, 1993.
de Beaulieu, J.-L.: Pollen Profile GPILXX, La Grande Pile, France, edited by: de Beaulieu, J.-L., Pangaea, European Pollen Database, 2010.
de Beaulieu, J. L., and Reille, M.: The last climatic cycle at La Grande Pile (Vosges, France) a new pollen profile, Quaternary Science Reviews, 11, 431-438, http://dx.doi.org/10.1016/0277-3791(92)90025-4, 1992.
Dorale, J. A., Liu, Z.: Limitations of Hendy test criteria in judging the paleoclimatic suitability of speleothems and the need for replication, Journal of Cave and Karst Studies, 71, 73-80, 2009.
Drysdale, R. N., Zanchetta, G., Hellstrom, J. C., Fallick, A. E., McDonald, J., and Cartwright, I.: Stalagmite evidence for the precise timing of North Atlantic cold events during the early last glacial, Geology, 35, 77-80, 2007.
Drysdale, R. N., Hellstrom, J. C., Zanchetta, G., Fallick, A. E., Sánchez Goñi, M. F., Couchoud, I., McDonald, J., Maas, R., Lohmann, G., and Isola, I.: Evidence for Obliquity Forcing of Glacial Termination II, Science, 325, 1527-1531, 2009.
Dutton, A., and Lambeck, K.: Ice Volume and Sea Level During the Last Interglacial, Science, 337, 216-219, 10.1126/science.1205749, 2012.
Edwards, R. L., Chen, J. H., Ku, T. L., and Wasserburg, G. J.: Precise Timing of the Last Interglacial Period from Mass Spectrometric Determination of Thorium-230 in Corals, Science, 236, 1547-1553, 1987.
Ehleringer, J. E., Cerling, T. E., Helliker, B. R., C4 photoynthesis, atmospheric CO2, and climate, Oecologia, 112, 285-299, 1997.
Fairchild, I. J., Smith, C. L., Baker, A., Fuller, L., Spotl, C., Mattey, D., McDermott, F., and Eimp: Modification and preservation of environmental signals in speleothems, Earth-Science Reviews, 75, 105-153, 10.1016/j.earscirev.2005.08.003, 2006.
Fairchild, I., and Baker, A.: Speleothem Science: from Process to Past Environments, Wiley-Blackwell, 2012.
Friedman, I., O'Neil, J., and Cebula, G.: Two New Carbonate Stable-Isotope Standards, Geostandards Newsletter, 6, 11-12, 10.1111/j.1751-908X.1982.tb00340.x, 1982.
Frisia, S.: Microstratigraphic logging of calcite fabrics in speleothems as tool for palaeoclimate studies, International Journal of Speleology, 44, 1-16, 10.5038/1827-806x.44.1.1, 2015.
Galaasen, E. V., Ninnemann, U. S., Irvali, N., Kleiven, H. F., Rosenthal, Y., Kissel, C., and Hodell, D. A.: Rapid Reductions in North Atlantic Deep Water During the Peak of the Last Interglacial Period, Science, 343, 1129-1132, 10.1126/science.1248667, 2014.
Gascoyne, M.: Paleoclimate determination from cave calcite deposits, Quaternary Science Reviews, 11, 609-632, 10.1016/0277-3791(92)90074-i, 1992.
Genty, D., Blamart, D., Ouahdi, R., Gilmour, M., Baker, A., Jouzel, J., and Van-Exter, S.: Precise dating of Dansgaard-Oeschger climate oscillations in western Europe from stalagmite data, Nature, 421, 833-837, 2003.Genty, D., Verheyden, S., and Wainer, K.: Speleothem records over the Last Interglacial, 1, PAGES, 24-25, 2013.
Gewelt, M., and Ek, C.: Les Concrétions Carbonatees des Grottes: aperçu synthetique, Annales de la Société géologique de Belgique, 111, 9-19, 1988.
Gimeno, L., Drumond, A., Nieto, R., Trigo, R. M., Stohl, A.: On the origin of continental precipitation, Geophysical Research Letters, 37, L13804, doi:10.1029/2010GL043712, 2010.
Goelzer, H., Huybrechts, P., Loutre, M. F., and Fichefet, T.: Impact of ice sheet meltwater fluxes on the climate evolution at the onset of the Last Interglacial, Clim. Past Discuss., 11, 4391-4423, 10.5194/cpd-11-4391-2015, 2015.

Formatted: English (U.S.)
Formatted: Normal, Justified, Line spacing: single
Formatted: English (U.S.)

Hearty, P. J., Hollin, J. T., Neumann, A. C., O'Leary, M. J., and McCulloch, M.: Global sea-level fluctuations during the Last Interglaciation (MIS 5e), Quaternary Science Reviews, 26, 2090-2112, 10.1016/j.quascirev.2007.06.019, 2007.

Helmens, K. F.: The Last Interglacial Glacial cycle (MIS 5-2) re-examined based on long proxy records from central and northern Europe, Quaternary Science Reviews, 86, 115-143, 10.1016/j.quascirev.2013.12.012, 2014.

Hendy, C. H.: Isotopic geochemistry of speleothems. 1. Calculation of effect of different modes of formation on isotopic compositions of speleothems and their applicability as paleoclimatic indicators, Geochimica Et Cosmochimica Acta, 35, 801-824, 10.1016/0016-7037(71)90127-x, 1971.

Holzkamper, S., Mangini, A., Spotl, C., and Mudelsee, M.: Timing and progression of the Last Interglacial derived from a high alpine stalagmite, Geophysical Research Letters, 31, 4, 10.1029/2003gl019112, 2004.

Irvali, N., Ninnemann, U. S., Galaasen, E. V., Rosenthal, Y., Kroon, D., Oppo, D. W., Kleiven, H. F., Darling, K. F., and Kissel, C.: Rapid switches in subpolar North Atlantic hydrography and climate during the Last Interglacial (MIS 5e), Paleoceanography, 27, 16, 10.1029/2011pa002244, 2012.

Kukla, G. J., Bender, M. L., de Beaulieu, J. L., Bond, G., Broecker, W. S., Cleveringa, P., Gavin, J. E., Herbert, T. D., Imbrie, J., Jouzel, J., Keigwin, L. D., Knudsen, K. L., McManus, J. F., Merkt, J., Muhs, D. R., Muller, H., Poore, R. Z., Porter, S. C., Seret, G., Shackleton, N. J., Turner, C., Tzedakis, P. C., and Winograd, I. J.: Last interglacial climates, Quaternary Research, 58, 2-13, 10.1006/qres.2002.2316, 2002.

Lachniet, M. S.: Climatic and environmental controls on speleothem oxygen-isotope values, Quaternary Science Reviews, 28, 412-432, 10.1016/j.quascirev.2008.10.021, 2009.

Loutre, M. F., Fichefet, T., Goosse, H., Huybrechts, P., Goelzer, H., and Capron, E.: Factors controlling the last interglacial climate as simulated by LOVECLIM1.3, Clim. Past, 10, 1541-1565, 10.5194/cp-10-1541-2014, 2014.

Martinson, D. G., Pisias, N. G., Hays, J. D., Imbrie, J., Moore, T. C., and Shackleton, N. J.: Age dating and the orbital theory of the ice ages: Development of a high-resolution 0 to 300,000-year chronostratigraphy, Quaternary Research, 27, 1-29, http://dx.doi.org/10.1016/0033-5894(87)90046-9, 1987.

McDermott, F.: Palaeo-climate reconstruction from stable isotope variations in speleothems: a review, Quaternary Science Reviews, 23, 901-918, http://dx.doi.org/10.1016/j.quascirev.2003.06.021, 2004.

McDermott, F., Atkinson, T. C., Fairchild, I. J., Baldini, L. M., and Mattey, D. P.: A first evaluation of the spatial gradients in delta O-18 recorded by European Holocene speleothems, Global and Planetary Change, 79, 275-287, 10.1016/j.gloplacha.2011.01.005, 2011.

McManus, J. F., Bond, G. C., Broecker, W. S., Johnsen, S., Labeyrie, L., and Higgins, S.: High-resolution climate records from the North Atlantic during the last interglacial, Nature, 371, 326-329, 1994.

Meyer, M. C., Spotl, C., and Mangini, A.: The demise of the Last Interglacial recorded in isotopically dated speleothems from the Alps, Quaternary Science Reviews, 27, 476-496, 10.1016/j.quascirev.2007.11.005, 2008.

Moseley, G. E., Spötl, C., Cheng, H., Boch, R., Min, A., and Edwards, R. L.: Termination-II interstadial/stadial climate change recorded in two stalagmites from the north European Alps, Quaternary Science Reviews, 127, 229-239, http://dx.doi.org/10.1016/j.quascirev.2015.07.012, 2015.

NEEM community: Eemian interglacial reconstructed from a Greenland folded ice core, Nature, 493, 489-494, 10.1038/nature11789, 2013.

NGRIP members.: High-resolution record of Northern Hemisphere climate extending into the last interglacial period, Nature, 431, 147-151, 2004.

Otto-Bliesner, B. L., Rosenbloom, N., Stone, E. J., McKay, N. P., Lunt, D. J., Brady, E. C., and Overpeck, J. T.: How warm was the last interglacial? New model - data comparisons, Philosophical Transactions of the Royal Society A: Mathematical, Phys. Engin. Sci., 371, 1–20, 2013.

Otvos, E. G.: The Last Interglacial Stage: Definitions and marine highstand, North America and Eurasia, Quaternary International, 383, 158-173, http://dx.doi.org/10.1016/j.quaint.2014.05.010, 2015.

Petit, J. R., Jouzel, J., Raynaud, D., Barkov, N. I., Barnola, J. M., Basile, I., Bender, M., Chappellaz, J., Davis, M., Delaygue, G., Delmotte, M., Kotlyakov, V. M., Legrand, M., Lipenkov, V. Y., Lorius, C., Pepin, L., Ritz, C., Saltzman, E., and Stievenard, M.: Climate and atmospheric history of the past 420,000 years from the Vostok ice core, Antarctica, Nature, 399, 429-436, 10.1038/20859, 1999.

Pyankov, V. I., Ziegler, H., Akhani, H., Deigele, C., Lüttge, U.: European plants with C4 photosynthesis: geographical and taxonomic distribution and relations to climate parameters, Botanical Journal of the Linnean Society, 163, 283-304, 2010.

Quinif, Y., and Bastin, B.: Datation Uranium/Thorium et Analyse Pollinique d'une Séquence Stalagmitique du Stade 5 (Galerie des Verviétois, Grotte de Han-sur-Lesse, Belgique), Comptes Rendus de l'Académie des Sciences, 318, 211-217, 1994.

Quinif, Y.: Complex stratigraphic sequences in Belgian caves: correlation with climate changes during the Middle, the Upper Pleistocene and the Holocene. , Geologica Belgica, 9, 231-244, 2006.

Rasmussen, S. O., Bigler, M., Blockley, S. P., Blunier, T., Buchardt, S. L., Clausen, H. B., Cvijanovic, I., Dahl-Jensen, D., Johnsen, S. J., Fischer, H., Gkinis, V., Guillevic, M., Hoek, W. Z., Lowe, J. J., Pedro, J. B., Popp, T., Seierstad, I. K., Steffensen, J. P., Svensson, A. M., Vallelonga, P., Vinther, B. M., Walker, M. J. C., Wheatley, J. J., Winstrup, M.: A stratigraphic framework for abrupt climatic changes during the Last Glacial period based on three synchronized Greenland ice-core records: refining and extending the INTIMATE event stratigraphy, Quaternary Science Reviews, 106, 14-28, 2014.

Riechelmann, D. F. C., Schroeder-Ritzrau, A., Scholz, D., Fohlmeister, J., Spoetl, C., Richter, D. K., Mangini, A.: Monitoring Bunker Cave (NW Germany): A prerequisite to interpret geochemical proxy data of speleothems from this site, Journal of Hydrology, 409, 682-695, 2011.

Rozanski, K., Araguasaraguas, L., and Gonfiantini, R.: Relation between long-term trends of 18-O isotope composition of precipitation and climate, Science, 258, 981-985, 10.1126/science.258.5084.981, 1992.

Sánchez Goñi, M. F., Eynaud, F., Turon, J. L., and Shackleton, N. J.: High resolution palynological record off the Iberian margin: direct land-sea correlation for the Last Interglacial complex, Earth and Planetary Science Letters, 171, 123-137, http://dx.doi.org/10.1016/S0012-821X(99)00141-7, 1999.

Sánchez Goñi, M. F., Bakker, P., Desprat, S., Carlson, A. E., Van Meerbeeck, C. J., Peyron, O., Naughton, F., Fletcher, W. J., Eynaud, F., Rossignol, L., and Renssen, H.: European climate optimum and enhanced Greenland melt during the Last Interglacial, Geology, 40, 627-630, 10.1130/g32908.1, 2012.

Scholz, D., and Hoffmann, D. L.: StalAge - An algorithm designed for construction of speleothem age models, Quaternary Geochronology, 6, 369-382, 10.1016/j.quageo.2011.02.002, 2011.

Schubert, B. A., and Jahren, A. H.: The effect of atmospheric CO2 concentration on carbon isotope fractionation in C3 land plants, Geochimica et Cosmochimica Acta, 96, 29-43, http://dx.doi.org/10.1016/j.gca.2012.08.003, 2012.

Shackleton, N. J.: Last Interglacial in marine and terrestrial records, Proceedings of the Royal Society Series B-Biological Sciences, 174, 135-+, 10.1098/rspb.1969.0085, 1969.

Shen, C. C., Wu, C. C., Cheng, H., Edwards, R. L., Hsieh, Y. T., Gallet, S., Chang, C. C., Li, T. Y., Lam D. D., Kano, A., Hori, M., Spötl, C.: High-precision and high-resolution carbonate 230Th dating by MC-ICP-MS with

Formatted: Normal, Justified, Line spacing: single

Formatted: English (U.S.)

Formatted: Normal, Justified, Line spacing: single

Formatted: English (U.S.)

SEM protocols, Geochimica et Cosmochimica Acta, 99, 71-86, 2012.

Sirocko, F., Seelos, K., Schaber, K., Rein, B., Dreher, F., Diehl, M., Lehne, R., Jager, K., Krbetschek, M., and Degering, D.: A late Eemian aridity pulse in central Europe during the last glacial inception, Nature, 436, 833-836, 2005.

Soreng, R. J., Peterson, P. M., Romaschenko, K., Davidse, G., Zuloaga, F. O., Judziewicz, E. J., Filgueiras, T. S., Davis, J. I., Morrone, O.: A worldwide phylogenetic classification of the Poaceae (Gramineae), Journal of Systematics and Evolution, 53(2), 117-137, 2015.

Timperman, M.: La Grotte de Han: Au Fil de Siècles, Gembloux, 66 pp., 1989.

Tzedakis, P. C., Frogley, M. R., and Heaton, T. H. E.: Last Interglacial conditions in southern Europe: evidence from Ioannina, northwest Greece, Global and Planetary Change, 36, 157-170, http://dx.doi.org/10.1016/S0921-8181(02)00182-0, 2003.

van Kreveld, S., Sarnthein, M., Erlenkeuser, H., Grootes, P., Jung, S., Nadeau, M. J., Pflaumann, U., and Voelker, A.: Potential links between surging ice sheets, circulation changes, and the Dansgaard-Oeschger Cycles in the Irminger Sea, 60–18 Kyr, Paleoceanography, 15, 425-442, 10.1029/1999PA000464, 2000.

Van Rampelbergh, M., Verheyden, S., Allan, M., Quinif, Y., Keppens, E., and Claeys, P.: Monitoring of a fast-growing speleothem site from the ~~Han-sur-Lesse cave~~Han-sur-Lesse Cave, Belgium, indicates equilibrium deposition of the seasonal δ18O and δ13C signals in the calcite, Clim. Past, 10, 1871-1885, 10.5194/cp-10-1871-2014, 2014.

Van Rampelbergh, M., Verheyden, S., Allan, M., Quinif, Y., Cheng, H., Edwards, L. R., Keppens, E., and Claeys, P.: A 500-year seasonally resolved δ18O and δ13C, layer thickness and calcite aspect record from a speleothem deposited in the ~~Han-sur-Lesse cave~~Han-sur-Lesse Cave, Belgium, Clim. Past, 11, 789-802, 10.5194/cp-11-789-2015, 2015.

Verheyden, S., Baele, J. M., Keppens, E., Genty, D., Cattani, O., Hai, C., Edwards, L., Hucai, Z., Van Strijdonck, M., and Quinif, Y.: The proserpine stalagmite (~~Han-sur-Lesse cave~~Han-sur-Lesse Cave, Belgium): Preliminary environmental interpretation of the last 1000 years as recorded in a layered speleothem, Geologica Belgica, 9, 245-256, 2006.

Verheyden, S., Genty, D., Deflandre, G., Quinif, Y., and Keppens, E.: Monitoring climatological, hydrological and geochemical parameters in the Pere Noel cave (Belgium): implication for the interpretation of speleothem isotopic and geochemical time-series, International Journal of Speleology, 37, 221-234, 2008.

Verheyden, S.: The 8.2 ka event: is it registered in Belgian speleothems?, Speleogenesis and Evolution of Karst Aquifers, 3-8, 2012.

Verheyden, S., Keppens, E., Quinif, Y., Cheng, H. J., and Edwards, L. R.: Late-glacial and Holocene climate reconstruction as inferred from a stalagmite - Grotte du Pere Noel, Han-sur-Lesse, Belgium, Geologica Belgica, 17, 83-89, 2014.

Waelbroeck, C., Labeyrie, L., Michel, E., Duplessy, J. C., McManus, J. F., Lambeck, K., Balbon, E., and Labracherie, M.: Sea-level and deep water temperature changes derived from benthic foraminifera isotopic records, Quaternary Science Reviews, 21, 295-305, 10.1016/s0277-3791(01)00101-9, 2002.

Wainer, K., Genty, D., Blamart, D., Bar-Matthews, M., Quinif, Y., and Plagnes, V.: Millennial climatic instability during penultimate glacial period recorded in a south-western France speleothem, Palaeogeography Palaeoclimatology Palaeoecology, 376, 122-131, 10.1016/j.palaeo.2013.02.026, 2013.

Wang, Y. J., Cheng, H., Edwards, R. L., An, Z. S., Wu, J. Y., Shen, C. C., and Dorale, J. A.: A High-Resolution Absolute-Dated Late Pleistocene Monsoon Record from Hulu Cave, China, Science, 294, 2345-2348, 2001.

Wohlfarth, B.: A review of Early Weichselian climate (MIS 5d-a) in Europe, Swedish Nuclear Fuel and Waste

Management Co, 2013.

Woillard, G. M.: Grande Pile peat bog: A continuous pollen record for the last 140,000 years, Quaternary Research, 9, 1-21, http://dx.doi.org/10.1016/0033-5894(78)90079-0, 1978.

Wong, C. I., and Breecker, D. O.: Advancements in the use of speleothems as climate archives, Quaternary Science Reviews, 127, 1-18, http://dx.doi.org/10.1016/j.quascirev.2015.07.019, 2015.

Yuan, D., Cheng, H., Edwards, R. L., Dykoski, C. A., Kelly, M. J., Zhang, M., Qing, J., Lin, Y., Wang, Y., Wu, J., Dorale, J., An, Z., Cai, Y.: Timing, Durqtion and Transition of the Last Interglacial Asian Monsoon, Science, 304, 575-578, 2004.

Point-by-Point reply to the comments

Both reviews treated separately. In black: suggestions made by the reviewers, in red: revised text, added text or comment made by the authors.

REVIEW #1

Specific Comments

Line 16 - the larger European spatial coverage of last interglacial climate records does not need to come specifically from speleothems, consider revising.

Changed to: To better understand regional climate changes over the past, a larger spatial coverage of European last interglacial continental records is essential and speleothems, because of their ability to obtain excellent chronologies, can provide a major contribution

Line 20 – Just because speleothems growing before 125.3 ka haven't been found yet, doesn't mean that they don't exist. Consider revising the bit about "speleothem formation starting relatively late in Belgium".

Changed to: The speleothem started growing relatively late within the last interglacial, at 125.3 ka, as other European continental archives suggest that Eemian optimum conditions were already present during that time.

Line 30 –Greenland stadials are not recognized in the Belgian speleothem, rathermore, stadials occurred in Belgium that appear to be analogous to those in Greenland.

Changed to: Stadials that appear to be analogous to those in Greenland are recognized in Han-9 and the chronology is consistent with other European (speleothem) records.

Line 31 – The last sentence needs revising. The second half related to Greenland Stadial 24 is fine, but the first half related to Greenland Stadial 25 is confusing. It is not clear that the Han-9 data is being referred to.

Changed to: Greenland Stadial 25 is reflected as a cold/dry period within Han-9 stable isotope proxies and the second interruption in speleothem growth occurs simultaneously with Greenland Stadial 24.

The first sentence of the introduction doesn't read well and needs revising. The higher temperature during the last interglacial also needs a reference.

Changed to: The last interglacial (LIG) period is known as the time interval before the last glacial period during which temperatures were similar to or higher than those of the Holocene period and Present Day (Otto-Bliesner et al., 2013).

Line 49 – the relationship between the two papers cited in this sentence is unclear.
Changed to: The term "Eemian" was originally introduced by Harting (1875) and was characterized by the occurrence of warm water mollusks in marine sediments of the Eem River valley, near Amsterdam, the Netherlands.

Line 51 – I'm not sure that amelioration is the right word to use here
Changed to: Nowadays, the Eemian is mostly interpreted as an interval of warmer climate associated with the spread of temperate mixed forests in areas with similar vegetation to today (Kukla et al., 2002).

Line 59 – the orbital parameters were different to what?
Changed to: Therefore, the LIG gained a lot of attention from both paleoclimate and climate modelling communities for studying a warmer climate state and potential future sea-level rise (Loutre et al., 2014; Goelzer et al., 2015), even though the present-day configuration of Earth's orbital forcing parameters is different (Berger and Loutre, 2002).

Line 62 – D/O cycles don't control climate variability, they are a feature of it.
Changed to: A major feature of climate variability during the last glacial is the occurrence of millennial-scale, rapid cold-warm-cold cycles, known as Dansgaard-Oeschger (D/O) events (Bond et al., 1993).
Lines 63-66 – Perhaps alternating would be a better word than succession? Nevertheless, the sentence needs revising. Atlantic Cold Events don't relate to the whole D/O cycle, plus the Atlantic Cold Events need a reference.
Changed to: These D/O cycles are expressed as alternating Greenland stadial (GS) and interstadial (GIS) phases in Greenland ice cores (Dansgaard et al., 1993; NGRIP members, 2004) and they also have affinity with Atlantic cold events registered in sea-surface temperature proxies (McManus et al., 1994).

Line 70 – gradual cooling of what?
Changed to: Nevertheless, according to Barker et al. (2015), it is more likely a non-linear response of a gradual cooling of the climate than a result of enhanced fresh-water input by iceberg calving, as previously proposed by Bond et al. (1995) and van Kreveld et al. (2000).

Line 95 – move the specifics about the length of the stalagmite to the cave setting. Then give more details about the sampling site. Average diameter? In situ or ex situ? Broken or complete? Refer to Fig 2C.
Added to section 2: Han-9, the stalagmite presented in this study, was deliberately sampled because it was already broken into three parts, so no other speleothems had to be destroyed. Although the sample was broken, it was still in situ. The candle-shaped stalagmite has a length of 70cm (Fig. 2C-E).

Line 108 – the rainfall is spread evenly throughout the year? Where does it come from? The same source all year? What is the modern d18O of the rainfall?
Changed to and addition of: . The amount of precipitation does not follow a seasonal distribution (Royal Meteorological Institute, RMI). The dominant moisture source in northwestern Europe is the North Atlantic Ocean, and this remains constant throughout the year (Gimeno, 2010). Modern δ18O of rainfall seasonally varies between -17‰ in winter and -4‰ in summer (Van Rampelbergh et al., 2014).

Line 114 – natural connection with which other parts of the cave? Perhaps indicate the underwater parts on the cave survey.
Changed to: The natural connection between the Réseau Sud and other parts of the Han-sur-Lesse Cave is fully submerged, but in 1960 an artificial tunnel was established facilitating access (Timperman, 1989).

Line 113-114. Rephrase. The sample can't have been collected in the Réseau Sud OR the southern network of Han-sur-Lesse
Changed to: The Han-9 stalagmite was collected within the Réseau Renversé, which is the most distal part of the Réseau Sud (Fig. 1B).

Line 115 – mark where the tunnel is on Fig. 1B.
It would be helpful to mark the position of Réseau Rénversé, Réseau Sud, Gouffre de Belveaux, Trou de Han on Fig. 1B
Figure 1B was revised. Locations mentioned in text were added, some information on original figure that was not relevant was removed.

The information about where the cave floods is confusing. Does flooding affect the sampling site?
Line 120 – when did the temperature logging take place? What were the sampling intervals?
Changed to: Temperature logging for six months with an interval of two hours in the Réseau Renversé shows an average cave temperature of 9.45°C with a standard deviation < 0.02°C, which reflects the average temperature of 9.2°C above the cave for 2013.

Line 121 – why does the cave temperature reflect the average temperature for 2013, rather than the 1999-2013 average? Does this have implications for the interpretation later on?
Reply: Temperature in the cave is stable and reflects the average year temperature above the cave.

The important point here is that the sample comes from the part of the cave with the stable temperature. Was that likely the same in the past? Or is there evidence for other entrances in the past that may have affected ventilation in this part of the cave?
Changed to: For the Réseau Renverse, there are no indications that cave morphology changed significantly since the last interglacial.

Line 137 – normally the half-lives are given as part of the U-Th data table. If you wish to give them in the text, why only give ^{230}Th and ^{234}U, and not the half-lives for the other relevant isotopes?
Reply: Half-lives were removed from text

Line 138 – specify atomic or activity ratio
Changed to: Ages were corrected assuming an initial 230Th/232Th atomic ratio of 4.4 ±2.2 x 10-6.

Line 139 – And also Shen et al., Geochimica et Cosmochimica Acta 99 (2012) 71–86
Reply: Reference was added

What is the age datum?
Added: The age datum is 1950 CE

Where were the stable isotopes measured?
Added: All stable isotope analysis were carried out at the Stable Isotope Laboratory, Vrije Universiteit Brussel.

Line 144 - 300µm diameter, radius, length?
Changed to: For all samples, tungsten carbide dental drill bits with a diameter of 300µm from Komet were used.

Line 145 – Revise sentence beginning "In function of the growth rate…". It is unclear what is meant.
Changed to: As a function of the growth rate, 1000, 500 and 250µm sampling resolutions were applied in order to maintain a more or less equal resolution in the time domain.

Line 146 - why were samples kept at 50°C
Changed to: Samples were kept at 50°C prior to analysis to avoid contamination

Line 149 – what is the in-house standard made from?
Changed to: Two samples of the in-house standard MAR-2(2), made from Marbella limestone and which has been calibrated against the international standard NBS-19 (Friedman et al., 1982), were measured every 10 samples to correct for instrumental drift.

Line 153 - do you mean replicate sample?
Changed to: At regular intervals, a replicate sample was measured in a different batch to check for the reproducibility of the analytical method.

Line 163 – it looks like the detrital material is on the base and not just the sides.
Changed to: In the lower 15mm, some fine, brown detrital laminae can be seen, although they are confined to the very base and the lateral sides of the stalagmite.

Line 163 onwards - it would help to be more specific about the sections of the speleothem being discussed. E.g. layering is visible between 365-700 mm dft.
Reply: The entire section 4.1. was revised to make it more clear.

How are the discontinuities identified? Macroscopically? By ages?
Changed to: This discontinuity was identified macroscopically.

Line 174 - …dashed lines in figure 2D….
Line 174 – do you mean no macroscopically visible internal layering is present?
Changed to: Besides some subtle unconformities marked by the dashed lines in Fig. 2D, no internal layering is visible macroscopically.

Lines 178-181 – You say that the latter fabric (i.e. the coarser one) has smaller columnar calcite crystals, thus you describe it as "columnar open". You then contradict yourself and say that the "coarser morphology has substantially larger crystals…..defined as columnar elongated".
Changed to: Variations in fabric occur between macroscopically defined 'denser' and 'coarser' calcite (Fig. 2E), where the latter has smaller columnar calcite crystals with significantly more inter-crystalline porosity often filled with fluid inclusions (Fig. 3B), and thereby described as columnar open. The denser morphology has substantially larger crystals with almost no pore space and can be defined as columnar elongated.

Line 183 – How can the smaller more equant calcite crystals also cover the fine layer of brown detrital material that is D2.
Changed to: There, the columnar fabric is replaced with smaller more equant calcite crystals (Fig. 3C), which are then followed by a fine layer of brown detrital material representing D2.

Later in section 5 there should be some discussion about why the morphology changes throughout the stalagmite. Why does the fabric change from dense to coarse? Why is there visible layering in some parts and not others. What might cause the growth axis to shift for 20mm?

Line 187 – The datum is given here as 2015 CE. Yet in the table it is 1950 AD.
Include some text in section 4.2 about the concentration and cleanliness of the samples.
Changed to: In all samples, the detrital Th content, estimated by 232Th concentration and the initial 230Th/232Th atomic ratio, is relatively low (range 6419 – 208 ppt). This leads to only minor corrections for the 230Th age (Table 1).

Line 197 – be more specific about the section of stalagmite
Do you have any idea why there are age inversions?
Changed to: Between 176 and 0mm dft, the distribution of the ages is more chaotic, with the occurrence of several age inversions and outliers.

Line 198 - What are the distinctive changes in morphology?
Lower amplitude variability in both δ13C and δ18O occur in the lower part of the stalagmite, and larger amplitude variations are present from ~400mm dft upwards, corresponding to distinct transitions in morphology (alternating zones of dense, more brown and coarser, more white calcite, Fig. 2E).

Line 199 – I think there should be some mention that the best test for isotopic equilibrium is to have a reproducible record (see Dorale and Liu, 2009). However, in the absence of a second speleothem, the Hendy test has been used instead. Do any of the modern monitoring studies record calcite deposition in isotopic equilibrium with the drip water?

Age model – why does the oldest part of the age model (figure 5) appear to miss out sample DAT-1? It is within stratigraphic order, yet the age model appears to completely miss it.

Reply: The entire part about Hendy tests was removed, as it is clear from review #2 that Hendy tests were not the best way to check for equilibrium deposition. In the discussion of the stable isotopes, a new section was added were covariation of stable isotopes is examined with Pearson's correlation coefficient. These coefficient were added in the new Table 2.

Added:

5.2.1 Isotopes deposited in isotopic equilibrium?

The best test for the presence of kinetic fractionation is to have a reproducible record (Dorale and Liu, 2009). However, in the absence of a second stalagmite record, Hendy tests could be performed (Hendy, 1971). The problem here is that growth rates are rather low and the layering very fine, so it would be hard to sample precisely in one layer. Therefore, an additional test for correlation of $\delta^{13}C$ and $\delta^{18}O$ was done by calculating the Pearson's correlation coefficient on the entire record and on the three growth phases separately (Table 2). Yet, a correlation between $\delta^{13}C$ and $\delta^{18}O$ does not give conclusive evidence for the presence of kinetic fractionation, as both $\delta^{13}C$ and $\delta^{18}O$ are expected to be controlled by climate and could therefore show positive or negative covariation (Dorale and Liu, 2009). The Pearson's coefficients reveal that there is a clear difference between the separate growth phases. The first growth phase, with $\rho = 0.024$, marks no covariation. The second growth phase, with $\rho = -0.467$, has a substantial degree of negative covariation, whereas the third growth phase ($\rho = 0.461$) has a positive covariation. The differences between the coefficients of the separate growth phases indicate that several processes are controlling the stable isotope variability and that the presence or absence of covariation reflects changes in climate conditions between the growth phases rather than the presence or absence of equilibrium. Nevertheless, equilibrium deposition between the drip water and recent calcite in Han-sur-Lesse Cave has been observed by Van Rampelbergh et al. (2014).

Lines 218-223 – Why does the age model need to be adjusted at the end of growth phase 2? Looking at the ages in table 1, DAT 6, 16 and 19 are all in stratigraphic order within the limits of dating uncertainty. Why then is there a discussion about whether DAT-19 is an outlier or not? Why has linear interpolation been applied at the end of growth phase 2? For this discussion, the names of the relevant samples should be added to figure 5.

Incidentally, it would be helpful to mark on one of the figures, either figure 2 or figure 5, what is meant by growth phases 1,2 and 3.

Reply: Figure 5 has been revised (now figure 4). Also, the entire discussion about the age model has been modified taking into account suggestions from review #1 and #2.

Changed to:

The StalAge algorithm (Scholz and Hoffmann, 2011) was applied to the individual ages in order to construct an age-depth model, displayed in Fig. 4. It is clear that the stalagmite endured three separate growth phases, and that the discontinuities, expressed in the stalagmite morphology at 302 and 176mm dft (Fig. 2D), correspond to two hiatuses separating these three growth phases. In the first growth phase, all ages are in stratigraphic order and are included within the model and the 2σ error. DAT-1 has only limited weight in the final model and an explanation for this is given in the algorithm specifications (Scholz and Hoffmann, 2011). During the modeling process, the StalAge algorithm has a step where the data is screened for the occurrence of minor outliers and age inversions. This is done by fitting error weighted straight lines through subsets of three adjacent data points. However, DAT-1 is located in the basal part of the stalagmite, so less subsets of three data points can be used including DAT-1. If DAT-1 does not fit on the error weighted straight line created with the adjacent data points DAT-10 and DAT-11, which is the case here, the error of DAT-1 will be increased and the weight of DAT-1 in the Monte Carlo simulation for the age fitting will decrease. This results in less solutions where DAT-1 is included in the Monte Carlo simulated age models. The occurrence of substantial changes in growth rate in the boundary areas of a speleothem sample is

recognized as a limitation of the StalAge algorithm (Scholz and Hoffmann, 2011). Even though the three growth phases were modeled separately with StalAge, the model does not perform well with the start of the Hiatus 2, as DAT-19 is completely excluded. Likely, this is again caused by the fact that DAT-19 is located in a boundary area. Here, the stalagmite petrography shows clear evidence of a significantly decreased growth rate after DAT-16 (110.6 ka), i.e. very dense, brownish calcite with fine laminae (Fig. 2C and E). In complex cases, such as in this study where multiple hiatuses occur, the simplest model is still the best. Therefore, linear interpolation combined with good observations of changes in petrography, was applied to include DAT-19 within the age model (Fig. 4, red line). For the third growth phase, because of the occurrence of several age inversions, the resulting age model is unreliable. Despite the fact that ages clearly cluster between ~103 and ~97 ka, the chronology of the third growth phase is only poorly constrained and therefore a detailed interpretation of Han-9 in terms of paleoclimate is limited to the first two growth phases. The first growth phase starts at 125.34 +0.78/-0.66 ka with stable growth-rate of 0.02mm yr-1 up to around 120.5 ka. After that, the growth rate significantly increases, with values up to 0.15mm yr-1. At 117.27 +0.69/-1.02 ka, growth ceases and the first hiatus, H1, starts. The hiatus lasts 4.41 +1.10/-1.49 ka and at 112.86 +0.47/-0.41 ka growth phase 2 starts. DAT-4 and DAT-5 were taken 6mm below and above the discontinuity and the age-depth model does not show any reason to question the timing of H1. As for the second growth phase, growth-rate remains at a constant pace of 0.04mm yr-1 until approximately 110.5 ka, where it decreases to 0.006mm yr-1. At 106.59 +0.21/-0.22 ka, the second growth phase ends. Given this age-depth model, stable isotopes were analyzed with a temporal resolution between 100 and 0.3 years, and an average of 16 years.

Lines 224-232 – Refer to figure 5 for the timing of growth phases. Where is the growth rate data plotted? What is the reason for the change in growth rate? What is the temporal range of the stable isotope sampling interval (i.e., not just the average).
Changed to: Given this age-depth model, stable isotopes were analyzed with a temporal resolution between 100 and 0.3 years, and an average of 16 years.

Line 235 – what is the reason for difference in d13C between modern and Han-9?
Lines 236-258 – This section on d13C needs some revision. The shift of 5‰ to enriched values in Han-9 is centred on c. 110 ka. How long does this isotopic excursion last for? Be more specific about when the grass assemblage at Eifel was at 40%. How reliable is the chronology on the maar lake record? After much discussion about the different factors that control d13C in speleothems, there is no decision as to which mechanism(s) are controlling d13C in this particular record. The end of section 5.2 concludes by saying that shifts in d13C are caused by changes in vegetation type. After assessing all the different causes of changes in d13C, why has this conclusion been reached? i.e., Why is prior calcite precipitation discarded? Furthermore, why is there a mismatch between the pollen record from Eifel and the d13C of Han-9 if changing vegetation is the control on d13C? Between c.126-114 ka broad leaf trees dominate the assemblage, hence one would expect a speleothem d13C of -6 to -14 ‰, and this is the case at c.-7‰. The enrichment in speleothem d13C is then in agreement with the decline in broad leaf trees and increase in grass assemblages. This is fine too. But then the speleothem d13C shifts to c. -9 ‰ after 109 ka, i.e. it is even more depleted than it was between 126-114 ka, yet at this time grasses are most abundant (60%) and trees much less (40%). If the shifts in speleothem d13C are really reflecting changes in vegetation, then the absolute d13C values and pollen assemblages from the maar lake are not in agreement.
Reply: Section about d13C has been revised

Line 260 – “precipitation” is a bit vague in terms of control on d18O. Perhaps use moisture source, amount effect.
Changed to: In mid-latitude Europe, several different processes (including temperature, amount effect and ocean source) influence speleothem δ18O variability (McDermott, 2004).

Lines 272-273 – "precipitation controls" is too vague. Do you mean amount? Is the North Atlantic Ocean the source for the precipitation all year round? And would it have been the source in the past?
Changed to: Temperature and precipitation (through the amount effect) controls are thus expected to contribute most to the speleothem δ18O variability

Added in section **2:** The dominant moisture source in northwestern Europe is the North Atlantic Ocean, and this remains constant throughout the year (Gimeno, 2010).

Line 276 – global d18O values of what?
Changed to: Waelbroeck et al. (2002) estimated that during MIS 5d, average global δ18O values of ocean waters were up to 0.5‰ higher compared to MIS 5e.

Lines 283-288 – be more specific about which sections of the d13C signal are controlled by the different mechanisms.
Reply: Paragraph was removed.

Lines 296-297 – The results presented here show quite clearly that speleothem deposition is not restricted to optimum interglacial conditions.
Changed to: Cave systems in Belgium are known to be very sensitive recorders of glacial/interglacial changes, with speleothem deposition only during interglacial intervals (Quinif, 2006).

Lines 316-317 – Be specific about why this demonstrates that interglacial conditions were already present at 125.3 ka.
Changed to: The low δ13C values perhaps demonstrate that interglacial optimum conditions were already present before 125.3 ka, but that an increase in moisture availability caused by enhanced precipitation above the cave, shown by the δ18O decrease, was the factor needed to trigger growth of Han-9.

Line 321 – refer to figure at end of first sentence
Changed to: The isotope records of Han-9 are relatively stable between 125 and ~120 ka (Fig. 5).

Line 324-326 – revise sentence so that the time period that is being referred to is clear
Changed to: The long-term trend, as displayed by a fitted 7-point running average (Fig. 5), shows lower variability between 125 and ~120 ka, especially when compared to younger growth periods of Han-9 (i.e. 120-117.3 ka and 112.9-106.6 ka).

Line 329 – refer to figure 7 at end of list about speleothems and ice cores
Changed to: During 125-120 ka, other paleoclimate records display stable interglacial conditions, such as speleothems from the Alps (Meyer et al., 2008; Moseley et al., 2015) and from Italy (Drysdale et al., 2009), and other archives including ice cores (NEEM community, 2013) (Fig. 5)

Line 331 – reference for enhanced Greenland melting
In marine records off the Iberian Margin, the 125-119 ka period was identified as an interval of 'sustained European warmth', following a time of enhanced Greenland melting between 131.5 and 126.5 ka (Sánchez Goñi et al., 2012).

Line 332 – you say there is a constant growth rate, but there are only three data points through which the age model passes over nearly a 9 cm interval. I come back to the earlier comment that the age for DAT-1 is completely ignored by the age model, despite being in stratigraphic order. If the age model took this age into account, then the growth rate would not be constant over the interval 120-125 ka.
Reply: No growth rate changes since original age model is retained.

Line 333 – no significant change in what over time? What is it about the layered calcite that indicates a stable climate?

Changed to: This is also supported by the constant growth rate (Fig. 4) and the speleothem morphology, displaying a sequence of layered calcite which does not show any significant change over the 125-120 ka period (Fig. 2C-E).

Line 336 – refer to figure at end of first sentence.

Line 336 – don't use "onwards", be specific about the time interval being discussed. This is important for the sentence where it is stated that no major changes in d13C are observed. Major changes take place at 117.5 ka (as is discussed in the next paragraph), and this is "onwards" of 120 ka. Line 336-337 – This needs rewording. At 120 ka, there is indeed an enrichment in d18O of 0.5‰, and the growth rate does change at this point, but the reduction in diameter doesn't appear to happen until later within this growth period. Also refer to figure 2 regarding growth diameter.

Changed to: At 120 ka, an increase in δ18O of 0.5‰ is observed (Fig. 5). This change in δ18O of the speleothem corresponds with an elevated growth rate (Fig. 4) and a speleothem morphology that becomes progressively coarser, with layers that are less expressed (Fig. 2C and E).

Line 336-352 – In the results section there was a lot of text about the d18O being controlled predominantly by temperature, but in this section it has now switched to both amount and source effect. Also, why does it switch from amount to source?

Line 355 – the sentence beginning "As the increase…." isn't complete. It is only the first part of a thought. What is happening as a result of the increase in d13C?

Changed to: The increase in δ13C here is believed to reflect changes in vegetation, such as an increase grasses resulting in lower vegetation activity, linked to a changing (drying and/or cooling) climate.

Line 358-361 – yes the beginning of the hiatus takes place within GS 26, but the age 117.3 ka doesn't stand out as a particular event within Greenland. GS-26 began at 119.1 ka (Rasmussen et al., 2014)

Not changed: First of all, in the NGRIP δ18O record it falls within what is identified as Greenland Stadial 26 (NGRIP Members, 2004). Although the signature of this GS may not be as clear as the younger GS 25 or 24, it corresponds with the overall decreasing trend observed in the ice δ18O, and also recognized in the more recent NEEM ice core (NEEM community, 2013).

Line 370-371 – add the Meyer et al 2008 data to figure 7.

Reply: Figure was revised (now figure 5) and Meyer et al 2008 was added.

Hiatus 1 – boreal forests recover after the LEAP event, but the speleothem doesn't start growing until much later. Please comment.

Added in section 5.3.4: The LEAP event in the Eifel maar only lasts 468 years (Sirocko et al., 2005), yet speleothem growth does not recover immediately after the LEAP event. A similar observation was made for the start of speleothem growth at 125.3 ka: optimum conditions were already present before Han-9 started growing. From this delayed growth, it appears that climate conditions need to be more favorable (warmer/wetter) to initiate growth than to sustain growth.

Line 390 – use the GICC05modelext timescale rather than GICC05

Line389 – in Rasmussen et al 2014, GS 25 is 110.6 to 108.3 ka

Changed to: The maximum in δ13C and the minimum in δ18O correspond well with the timing of GS 25 (110.6-108.3 ka, Rasmussen et al., 2014) observed in the NGRIP record (plotted on the GICC05modelext timescale), implying that the stable isotopes of Han-9 reflect the temperature decrease of the stadial, which is likely since higher δ13C is linked to a less active vegetation cover during colder periods (i.e. more grasses) and lower δ18O is caused by lower temperatures.

Line 396 – there is a different timing here for GS25 compared to line 389

Line 396 – suggesting what is mainly temperature controlled?

Changed to: Between 112.9 and 111 ka, the variability of δ13C and δ18O in Han-9, predating GS 25, has an inverse relationship suggesting that δ18O is mainly temperature controlled.

Line 400-401- Rephrase the question. You ask why speleothem growth continued during GS 25, but then answer why it stopped during GS24.
Changed to: However, if the hiatus has any affinity with GS 24, this raises the question why speleothem growth stopped during GS 24 and continued during GS 25. A plausible explanation could be that growth never fully recovered from the GS 25, and that less favorable conditions (cooler/dryer) during the GS 24 interval were sufficient to cease growth.

Line 404 – Growth rate decreased at the same time d18O increased (amount effect=less rainfall), but d13C decreased
Reply: Adressed in the section about stable isotopes

Line 411-412- weak ending. Yes the age model is poorly constrained, but the ages clearly cluster within the interval 97-103.6 ka, hence, the more depleted d13C appears to be in good agreement with the high abundance of grasses. Perhaps it is a problem with the Eifel Maar chronology, rather than the U-Th chronology? You should discuss whether PCP or fractionation effects might be responsible.
Reply: Last part about growth phase three is removed, the depleted d13C (and PCP) is addressed in d13C section (5.2.2)

Technical corrections
General comments – There are many issues related to grammar, use of articles, prepositions, language, and in-house standards. Please address them.
All suggested technical corrections in text were carried out.

REVIEW #2

General Comments
Section 4.1 Speleothem morphology: This entire section is rather unclear.

The U/Th dates between 0 and 176 mm dft are unusable. I recommend not interpreting your record past Hiatus 2.

I lack confidence in the Hendy Tests (see Dorale and Lu, 2009). The first potential problem is that the drill bit is 300 microns and the reported growth rates are 20, 40 and 150 microns. This suggests that at worst the authors are averaging 15 years and at best, 2 years. Another potential explanation for the very flat Hendy Test results for d13C is that these tests only extend to 15 mm from the central growth axis which is likely within the splash cup and not enough distance (even under conditions of kinetic fractionation) for degassing to occur as the drip progresses toward the flanks. Also, the variability in the d18O data along a (presumably) single growth axis is nearly 25 % of the total d18O variability through time. This is less than inspiring. I suggest that a better test for kinetic fractionation is to look at how d18O and d13C covary (or anticorrelate) over the length of the record. Superficially I did this and it appears that there are intervals of strong anticorrelation such as during the 'Eemian

Optimum' and other periods of covariation such as after Hiatus II. Perhaps a running Pearson's could shed some light on when conditions favoured kinetic fractionation and this in itself provides valuable climate information. The presence of kinetic fractionation really only comes into play when aiming to apply the palaeotemperature equation. If this is not the goal (and I believe it is not here) then the presence or absence of kinetic fractionation does not rule out but can contribute information to the overall palaeoclimate interpretation.

Reply: In Section 4.3 (Results – Stable isotopes) the part about the Hendy test was removed, as well as Figure 4. This has been replaced by the Pearson's test in the discussion section. Within the discussion section, a new sub-division was made between equilibrium deposition – d13C – d18O.

For the Age Model, the authors might want to try COPRA to see if it handles the hiatuses better. Did the authors run StalAge over the two growth intervals separately? I don't see why StalAge would interpolate incorrectly over the last 2 dates in Growth Phase II if it were run over the two growth intervals separately. I suggest that short of trying COPRA, the authors should rerun StalAge over Growth Interval II alone and see if the age model is more true to the U/Th dates and errors over that interval. I think that the current linear interpolation is unsatisfactory. Again, I would limit discussion of Growth Phase III due to dating uncertainties.

Reply: Section 5.1 (Discussion – age model) has been completely revised and major issues, as addressed in the authors comment , were added. Also the figure has been revised.

Section 5.3 'A late onset of the Eemian' seems to be special pleading. Han-9 begins growing during the Eemian….in fact, well into it. I don't think there is enough evidence to support a late onset and would delete any of the discussion to this effect.

Changed to: 5.3 125.3 ka: Start of speleothem growth triggered by an increase in moisture availability

Discussion of controls on Han-9 d18O: 1) Lower T will cause lower d18O due to rainout, distillation, etc. 2) ice build-up will sequester 16O, leaving behind a higher ocean d18O (source moisture) and driving rainfall d18O higher, 3) lower T would cause lower in-cave T and drive stalagmite d18O higher (Craig equation) but this effect is trivial. Effects 1 and 2 act against each other but one would win out (unless they cancel each other out entirely!). It is likely that lower T and increased rainout/fractionation will win, and rainfall (and thus Han-9 d18O) will be more negative during colder conditions. It seems that the authors are arguing both sides in the manuscript but they need to pick one interpretation that applies to the whole record.

Added in section 5.3.4: The ice build-up effect, displayed by the increase in δ18O between 120 and 117.3 ka, is cancelled out by the effect of lower temperature, causing a decrease in speleothem δ18O

It's interesting and somewhat puzzling that Han-9 growth seems to be restricted to intervals between Insolation max and mins but not during (i.e., no growth centred on 104, 115, and 127 kyr). It would be interesting to know if there is some explanation for this

.

The authors use 'ka' and 'kyr BP' in the manuscript. Select one and be consistent throughout.

Reply: Changed throughout

I find the match between Han-9 d13C and the pollen record particularly compelling at least until Growth Phase III when dating (and possibly the data) inaccuracies dominate.

I disagree with stating that the start of Hiatus I marks the 'end of the Eemian', (such as the authors have done in the Conclusions and possibly elsewhere), rather, the authors could state that Han-9 ceases growth (Hiatus I) at 117.3 kyr, before the end of the Eemian as recorded by other proxies (references) suggesting that a critical threshold was reached in which conditions no longer favoured Han-9 deposition. This was possibly linked to a change in vegetation dynamics.

Reply: Not changed. 117.3 ka is identified as the end of the Eemian in this study. Also, it corresponds to what other speleothem studies recognized as end of the Eemian (Meyer et al., 2008; Hölzkamper et al., 2004)

Enumerated Comments

All suggested technical corrections in text were carried out.

Figures

Figure 1: Location of core MD03-2664 was added in Fig. 1A. In Fig. 1B, the terms in the text were better displayed.

Figure 3: Figure 2d shows 6 thin sections. Which ones are shown here in A-C. Suggest labelling Fig. 2d more clearly so one can more easily cross reference Figs. 2d and 3 A-C.
In Fig. 2 the blue boxes and thin section labels are shown more clearly now. Locations of Hendy tests were taken out because these are left out in the text as well.

Figure 4: Hendy tests were left out.

Figure 5: The section after Hiatus 2 is almost unusable. The error envelope shown (grey shading) does not cover the entire interval of age inversions and increased dating error. This needs to be expanded to cover the whole interval. I recommend excluding this growth interval from your discussions/interpretations. There is nothing obvious in Table 1 to explain why the dating is so imprecise over this interval.
Also, in Figure 5, it would help if the authors would label the datapoints. The Age model discussion in section 5.1 refers to DAT-#'s quite a bit and it would help if the reader could make quick reference to a well-labelled Fig. 5.
Label Fig. 5 growth intervals and growth rates
Suggestions were taken into account. Fig. 5 is now Fig. 4.

Figure 6: This figure is redundant considering that the same data are provided in Figure 7. I suggest deleting. In Figure 7 just darken slightly the non-averaged d18O and d13C curves…they are a bit too light to see right now.
Figure 6 was removed.

Figure 7: This figure is not very well laid out and could be vastly improved. The Han-9 data is minimised with compressed axes while the previously published datasets are at the forefront. Consider compressing the published data and expanding the axes on the Han-9 isotope data. I suggest making all of the axes the same length.
It might be informative to move the Insolation record down over (or between) the Han-9 datasets.
The U-Series datapoints should be plotted on 2 lines only (or one when they are not overlapping). The way they are now, suggests that there is some monotonic increase through time. Misleading.
I suggest adding in the Yuan et al 2004 Dongge Cave data. I know this is a SE Asian Monsoon dataset but it tracks Greenland ice core data quite well and could help fill in some blanks.
Add interpretations to figure. For instance, along axes like Han-9 d13C add down arrows (towards heavier d13C values) labelled with 'increasing C4 plants', 'Colder/drier', and 'increasing PCP', 'decreasing soil bioproductivity'. For Han-9 d18O add down arrows (towards lighter d18O values) decreasing ice volume
Make certain that all axes are pointing in the correct direction regarding a uniform interpretation for the figure.
The authors highlight the hiatuses but not the actual climate info. I suggest just labelling the data breaks as 'Hiatus 1' and 'Hiatus 2' (if the authors choose to keep growth phase III), but using shaded rectangles and more obvious labelling to highlight the climatic episodes discussed in the text (i.e., the Eemian climatic optimum from 120 to 125). Perhaps helpful to the reader would be to have the climatic periods identified (for instance in Paragraph 1 of the Introduction) in horizontal shaded rectangles at the bottom of the figure below the pollen data.
In caption add d18O to 'NALPS speleothem record'. Add (SST) after 'Sea Surface Temperature' in B) if this is the first mention. Otherwise, just use SST.

I suggest adding in the Irvali et al 2012 Fig. 3 b MD03-2665 Planktonic d18O record to Fig. 7, possibly overlapping with the Sanchez and Goni SST record. There is a lot more detail in the Irvali record and it is discussed in the text.

Figure completely revised with suggestions from both reviewers.

Response to additional Editor comments:

Line 66-67: This sentence still makes no sense to me. What does it mean for D/O cycles to have "an affinity" to something? Please clarify.

Reply: The part "and have affinity to the cold events in the North Atlantic Ocean" was removed. The exact relation of the surface cooling and Greenland stadials is still debated, as mentioned further in the text.

You have stated in the methods that the 230Th/232Th ratio has been corrected with a certain value. Please provide a brief justification for the value chosen in the text.

Moved to results section and changed to: Atomic $^{230}Th/^{232}Th$ ranges between 1064 and 33652 × 10^{-6}. Because detrital Th is relatively low in all samples, ages were corrected assuming an initial bulk earth $^{230}Th/^{232}Th$ atomic ratio of 4.4 ±2.2 × 10^{-6}.

You have cited 3 papers for methods, yet some of these papers differ in their methods used. Can you please clarify which parts of the method come from which papers, e.g., the chemical separation of U and Th is described in XX whereas the instrumental method follows the procedure described in XX, etc.

Changed to: The applied method is based on the fundamental principles of U-Th dating and mass spectrometry on carbonates provided by Edwards et al. (1987). For state of the art improvements on sample preparation, MC-ICP-MS protocols and ^{230}Th and ^{234}U half-live values, see Shen et al. (2012) and Chen et al. (2013) and references therein.